or Research Center

Bethesda, MD 20084-5000

DTRC-SME-91-11 October 1991

Ship Materials Engineering Department

Research and Development Report

Effects of Cyclic Loading on the Deformation and Elastic-Plastic Fracture Behavior of a Cast Stainless Steel

by

J.A. Joyce

E.M. Hackett

C. Roe

DTRC-SME-91-11 Effects of Cyclic Loading on the Deformation and Elastic-Plastic Fracture Behavior of a Cast Stainless Steel

MAJOR DTRC TECHNICAL COMPONENTS

CODE 011 DIRECTOR OF TECHNOLOGY, PLANS AND ASSESSMENT

12 SHIP SYSTEMS INTEGRATION DEPARTMENT

14 SHIP ELECTROMAGNETIC SIGNATURES DEPARTMENT

15 SHIP HYDROMECHANICS DEPARTMENT

16 AVIATION DEPARTMENT

17 SHIP STRUCTURES AND PROTECTION DEPARTMENT

18 COMPUTATION, MATHEMATICS & LOGISTICS DEPARTMENT

19 SHIP ACOUSTICS DEPARTMENT

27 PROPULSION AND AUXILIARY SYSTEMS DEPARTMENT

28 SHIP MATERIALS ENGINEERING DEPARTMENT

DTRC ISSUES THREE TYPES OF REPORTS:

1. **DTRC reports, a formal series,** contain information of permanent technical value. They carry a consecutive numerical identification regardless of their classification or the originating department.

2. **Departmental reports, a semiformal series,** contain information of a preliminary, temporary, or proprietary nature or of limited interest or significance. They carry a departmental alphanumerical identification.

3. **Technical memoranda, an informal series,** contain technical documentation of limited use and interest. They are primarily working papers intended for internal use. They carry an identifying number which indicates their type and the numerical code of the originating department. Any distribution outside DTRC must be approved by the head of the originating department on a case-by-case basis.

NSW DTNSRDC 5602, 5 Rev. 2-88

David Taylor Research Center

Bethesda, MD 20084–5000

DTRC–SME–91–11 October 1991

Ship Materials Engineering Department

Research and Development Report

Effects of Cyclic Loading on the Deformation and Elastic-Plastic Fracture Behavior of a Cast Stainless Steel

by

J.A. Joyce

E.M. Hackett

C. Roe

CONTENTS

FIGURES

TABLES

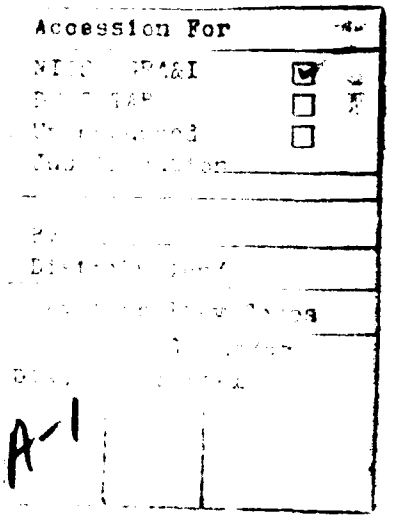

ABSTRACT

Tests conducted in Japan as part of the High Level Vibration Test (HLVT) program for reactor piping systems revealed fatigue crack growth in a cast stainless steel pipe elbow. The material tested was equivalent to ASME SA-351CF8M. The David Taylor Research Center (DTRC) was tasked to develop the appropriate material property data to characterize cyclic deformation, cyclic elastic-plastic crack growth and ductile tearing resistance in the pipe elbow material.

The tests conducted included monotonic and cyclic tensile tests, monotonic J-R curve tests, and cyclic elastic and elastic-plastic fatigue crack growth rate tests. The cyclic elastic-plastic fracture behavior of the stainless steel was of primary concern and was evaluated using a cyclic J-integral approach.

It was found that the cast stainless steel was very resistant to ductile crack extension. J-resistance curves essentially followed a blunting behavior to very high J levels. High cycle fatigue crack growth rate data obtained on this stainless steel was typical of that reported in standard textbooks. Low cycle fatigue crack growth rate data obtained on this material using the cyclic J integral approach was consistent with the high cycle fatigue crack growth rate and with a standard textbook correlation equation typical for this type of material. Evaluation of crack closure effects was essential to accurately determine the crack driving force for cyclic elastic-plastic crack growth in this material.

ADMINISTRATIVE INFORMATION

This work was performed at the David Taylor Research Center and the U.S. Naval Academy under the program, "Elastic-Plastic Fracture Mechanics Evaluation of LWR Alloys," E.M. Hackett, Program Manager. The program is sponsored by the Office of Nuclear Regulatory Research of the U.S. Nuclear Regulatory Commission (NRC). The technical monitors for the NRC were Mr. Michael Mayfield and Mr. Allen Hiser. This effort was undertaken in support of work being conducted by the Brookhaven National Laboratory (BNL) for the NRC under the program, "Analysis of Crack Initiation and Growth in the High Level Vibration Test at Tadotsu, Japan." The technical points of contact at BNL were Professor Mumtaz Kassir, Dr. Kamal Bandyopadhyay and Dr. Charles Hofmayer.

The HLVT project was performed by BNL and the Nuclear Power Engineering Center (NUPEC) in Japan as part of a nuclear power technical cooperative agreement between the USNRC and the Ministry of International Trade and Industry in Japan. The test results are reported in USNRC report NUREG/CR-5585.

INTRODUCTION

Tests conducted in Japan as part of the High Level Vibration Test (HLVT) program for reactor piping systems revealed fatigue crack growth in a cast stainless steel pipe elbow.[1] The material tested was equivalent to ASME SA-351CF8M. Upon detailed examination of the fracture surfaces from the HLVT elbow test, it was found that both fatigue and ductile tearing were present concurrently, leading to the postulate that the crack growth may have been "J-controlled." In support of analyses being conducted by the Brookhaven National Laboratory (BNL), the David Taylor Research Center (DTRC) was tasked to develop the appropriate material property data to characterize cyclic deformation, cyclic elastic-plastic crack growth and ductile tearing resistance in the pipe elbow material.

MATERIAL

CHEMISTRY

The chemistry of the HLVT elbow material was determined by DTRC and was found to meet specifications given for ASME A351 grade CF-8M. The results of the chemical analysis are presented in Table 1.

Table 1. Chemical Analysis of HLVT Program Stainless Steel Pipe Elbow

Element	Analysis	A351, CF-8M
Carbon	0.048	0.08 max.
Manganese	1.00	1.50 max.
Silicon	0.91	1.50 max.
Phosphorus	0.023	0.04 max.
Sulfur	0.004	0.04 max.
Chromium	17.8	18 to 21
Nickel	11.0	10 to 12
Molybdenum	2.09	2 to 3

METALLOGRAPHY

A macroetch was performed on a cross section of the pipe material using Marble's reagent (Fig. 1) in order to determine the details of the processing history. The grains were found to be elongated in the direction of the radial axis of the pipe cross section and curved in a fashion that is characteristic of a centrifugal casting.[2] Due to the irregularities in shape, an average grain size determination was impracticable.

TENSILE PROPERTIES

MONOTONIC

Round tensile specimens were prepared in a longitudinal orientation with respect to the pipe and tested in accordance with ASTM Standard E8. Three specimens had 0.505 inch (12.5 mm) diameters and 2 inch (51 mm) gage lengths, the remaining three specimens had 0.252 inch (6.4 mm) diameters and 1 inch (25 mm) gage lengths. The resulting tensile mechanical properties are presented in Table 2.

Table 2. Monotonic Tensile Properties of Cast Stainless Steel

Diameter (in.)	Yield Stress 0.2% Offset (ksi)	Ultimate Tensile Stress (ksi)	Fracture Stress (ksi)	Elongation (%)	Reduction in Area (%)
0.505	38.4	77.2	54.8	52	80
0.505	39.9	76.8	56.6	54	78
0.505	38.6	79.2	59.5	64	76
0.252	38.1	75.1	47.4	48	84
0.252	44.7	76.9	58.8	49	78
0.252	42.0	79.0	60.5	--*	--*

* Note: Specimen was necked outside the gage length, therefore the test was terminated and elongation and reduction in area could not be determined.

CYCLIC

Cyclic loading tensile properties were obtained on the material in the following manner. Standard round tensile specimens of 0.252 inch (6.4 mm) diameter and 1 inch (25 mm) gage length were axially, cyclically loaded to produce cyclic stress-strain curves as shown in Fig. 2. The initial displacement was taken to approximately 0.003 inch (0.08 mm), then the specimen was unloaded to zero load. Subsequent displacement steps consisted of increments of approximately 0.001 inch (0.025 mm). Data was taken continuously and stored in digital form. Each cycle had a duration of approximately six seconds, though this varied as the test proceeded because the specimen became more compliant as its area was reduced and its length increased. These results are presented in Figs. 2-4.

Specimens GPQ-33 and GPQ-36 were run until the 50% strain limit was reached on the strain transducer, while specimen GPQ-34 fractured outside the gage

length after a uniform strain of approximately 20% was achieved. These specimens demonstrated highly anisotropic and heterogeneous behavior as shown in Fig. 4.

The upper envelope of the cyclic stress strain curve is shown in Fig. 5 and compared to the results of static tensile tests. Fig. 5 shows that the cyclic loading tends to soften the material as far as ultimate strength is concerned and increase the apparent ductility. An exact comparison of the ductility, however, cannot be made since the cyclic tensile specimens were extended to the limit of the elongation transducer, hence not fractured.

MONOTONIC J-R CURVE BEHAVIOR

J-R curves were evaluated using the ASTM Standard E1152-87. The specimens used were 1T and 1/2T C(T) specimens according to E1152 with 1T specimens removed only in the L-C orientation (due to material thickness) and 1/2T specimens removed in both L-R and L-C orientations. A single specimen unloading compliance technique was utilized as described by Joyce and Gudas.[3] The resulting J-R curves are shown in Fig. 6. along with blunting line constructions of J = 2 * (flow stress) * (crack extension) and J = 4 * (flow stress) * (crack extension). It is clear from these results that this material follows a path between these blunting lines and does not fracture by ductile tearing, at least until well beyond the standard E1152 validity regions for 1/2T and 1T specimens. These validity regions are shown in Fig. 6 for comparison. This material is too tough to be characterized by the ASTM J-integral methods (E813-87 and E1152-87) using 1/2T or 1T specimens.

FATIGUE CRACK GROWTH RATE BEHAVIOR

LINEAR ELASTIC

The specimens prepared for fatigue crack growth rate (FCGR) testing were 1/2T C(T) specimens machined with integral knife edges for loadline crack-opening displacement (COD) measurements as shown in Fig. 7. The tests were run within the requirements of ASTM Standard E647-88a. A computer was used to estimate the crack growth using an elastic compliance equation for C(T) specimens. Tests were run in an increasing K mode at a constant frequency of 0.1 Hz and a minimum/maximum load ratio (R ratio) of 0.1. Data was stored digitally at increments of 0.010 inches (0.25 mm) of crack growth. Two specimens were tested, one in the L-C orientation, the other in the L-R orientation. The results of these tests are shown and compared to the Rolfe/Barsom[4] fatigue crack propagation equation for austenitic stainless steels in Fig. 8.

ELASTIC-PLASTIC

Cyclic J-testing was utilized to evaluate the crack growth resistance of the material under intense cyclic loading. It has been shown by several authors[5-8] that an operational J-integral range correlates the fatigue crack growth under cyclic growth conditions beyond that of linear elastic fracture mechanics as standardized by ASTM E647. In this work the load histories shown in Figs. 9-11 were used and will be referred to as R=0, R=0.3 and R=-1 load histories respectively. The "R=-1" case had, in fact, a range of negative R ratios, initially with $-1 < R < 0$, then for a few cycles with R=-1, and then for the remainder of the test, R was between -1 and -10 as the tensile load capacity of the specimen diminished.

The specimens used for these tests were 1/2T C(T) specimens, as previously described and shown in Fig. 7, with integral knife edges and 20% total side

grooves. Both L-R and L-C orientations were tested. Compression loading was applied to these specimens using fixtures known as load caps which are shown in Fig. 12. Basically, the clevis pin holes were toleranced such that on reversal of the test machine, load was applied to the specimen via the load caps instead of the loading pins. This system was a variant of that used by Joyce[8] for reversed loading cyclic fatigue/fracture tests, the improvement here was that the compression load caps stayed in place during both the compression and tensile loadings.

The J-integral was calculated on each cycle using the Merkle-Corten[9] J equation as modified by Clarke and Landes[10] to give:

$$J = \frac{\eta A}{B_n b}, \qquad (1)$$

with B_n = net specimen thickness,

b = (W-a) is the specimen's remaining ligament,

A = the area enclosed by the load-COD cyclic curve as described further below,

and $$\eta = 2[(1+\alpha)/(1+\alpha^2)], \qquad (2)$$

with $$\alpha = \{2(a/b)^2+2[2(a/b)]+2\}^{1/2}-[2(a/b)+1], \qquad (3)$$

The cyclic area was calculated as shown schematically in Fig. 13. The cyclic area, shown cross-hatched, is bounded by the loading portion of the load-COD curve, by a maximum COD vertical line and along the bottom by a crack closure load horizontal line. The critical calculation is to evaluate the crack closure load. This was done in this work by comparing the slope during

the initial cycle loading (k_I) with the slope of the first unloading portion of the previous cycle (k^*). The basic method is to fit a quadratic polynomial to the initial load versus COD data as:

$$P = A_1 + A_2\ COD + A_3\ COD^2. \qquad (4)$$

Then the slope is given by:

$$k_I = A_2 + 2A_3\ COD, \qquad (5)$$

and this can be set equal to the previous unloading slope, k^* to give:

$$k^* = k_I = A_2 + 2A_3\ COD. \qquad (6)$$

Solving for the closure COD gives:

$$COD^* = \frac{k^* - A_2}{2A_3}, \qquad (7)$$

and then P^* at closure can be evaluated from Eq. 4.

The crack length was evaluated for each cycle using the unloading compliance equations of ASTM E1152-87 including the rotation correction. For each load cycle the measured specimen compliance, crack length, correlation of the least squares fit and maximum COD were stored on magnetic disk. Also stored was a file giving load-COD pairs tracing out each cycle for post test processing for closure load, cyclic area and cyclic J.

DISCUSSION

CYCLIC J DATA

As described in the previous section, the specimen compliance was calculated while the test was in progress, the crack length was calculated, then stored and this process was repeated for each cycle. Only a small part of the data used to calculate the crack lengths was stored and these crack length estimates

were taken as the best measure of crack length for each cycle, i.e. they could not be improved by post test processing. Typical data is shown for four of the R=-1 specimens in Fig 14. Compliance estimates of crack length were generally very consistent and appeared repeatable to a precision of about +/- 0.001 inch (0.03 mm). For the R=-1 specimens, the initial and final compliance estimated crack lengths were shown to be accurate in comparison with 9-point average crack lengths measured optically from the specimen fracture surfaces after the test. These results are shown in Table 3. For the R=0 and R=0.3 specimens, the compliance estimates of crack extension, in some cases, were significantly less than the measured values. This was attributed to crack curvature (tunneling) which was observed on the specimen fracture surfaces and to failure of the crack rotation correction procedure to adequately account for the gross specimen deformation. Had the compliance and measured values been in closer agreement, more rapid fatigue crack growth rates would have been obtained.

Table 3. Estimated vs. Measured Crack Growth for Cyclic Crack Growth Rate Tests and J-R Curve Tests of Cast Stainless Steel

Test Condition	Specimen I.D.	Estimated Crack Growth (in.)	Measured Crack Growth (in.)
High Cycle Fatigue	GPQ-5	0.106	0.124
	GPQ-15	0.083	0.115
Cyclic J R=-1	GPQ-2	0.353	0.368
	GPQ-7	----- Not Available -----	
	GPQ-16	0.352	0.378
	GPQ-17	0.323	0.350
Cyclic J R=0.3	GPQ-8	0.091	0.123
	GPQ-20	0.095	0.151
Cyclic J R=0	GPQ-9	0.071	0.094
	GPQ-11	0.104	0.162
	GPQ-23	0.100	0.143
	GPQ-25	0.110	0.161
J-R Curve Tests	GPQ-38	0.112	0.119
	GPQ-39	0.113	0.130
	GPQ-3	0.038	0.050
	GPQ-12	0.040	0.047
	GPQ-18	0.035	0.030
	GPQ-19	0.039	0.026
	GPQ-26	0.025	0.030

The R=0 and R=0.3 cases did not appear to demonstrate a crack closure phenomena for this material, even for the most intense loading cycles. For these specimens, the minimum load on each cycle was taken as the lower bound load for the cyclic area and cyclic J calculation. The R=-1 case demonstrated crack closure and required the calculation of a closure load for each cycle before the cyclic area and cyclic J could be calculated. The method used for this was discussed in the previous section. Results for the four R=-1 specimens are shown in Fig. 15. At the beginning, the method generally finds a closure load near the minimum (compression) load in each cycle. Some variability is shown on Fig. 15 for specimen GPQ-16 for the first few cycles, but basically a rather steady, negative closure load is located before 25 cycles have been applied to the specimen. This closure load then remains nearly constant throughout the remaining cycles until the tensile load capacity is reached and the COD steps of 0.004 inch (0.1 mm) are applied. When this happens, the closure load returns toward zero load if the test is not terminated first due to COD transducer limitations.

The closure load of between -500 and -1000 lbs. is well above the -2500 lbs. minimum load applied to the R=-1 specimens. The use of the minimum load in the cyclic J calculation rather than the closure load would have dramatically increased the cyclic J values resulting in an erroneous calculation of the applied cyclic J.

Figures 16, 17 and 18 show cyclic J as a function of cycle count for the R=0, R=0.3 and R=-1 cases respectively. For the cyclic loading used here, the cyclic J range experienced by the R=0 and R=0.3 cases is very limited, while for the R=-1 case a wide range of cyclic J was sampled by each specimen. In all cases the cyclic J is seen to be a smooth function of cycle count which can be utilized to obtain a da/dN versus ΔJ fatigue crack growth rate

characterization of the material.

This final step is shown in Figs. 19-21 for the R=0, R=0.3 and R=-1 cases. Since the J range sampled by the R=0 and R=0.3 cases is limited, only limited fatigue crack growth data is obtained from each of these specimen taken independently. A combined plot showing one specimen of each orientation and R ratio is shown in Fig. 22. It is clear that the R=0 and R=-1.0 data sets define a single power law relationship while the R=0.3 seems to demonstrate somewhat accelerated crack growth. The excellent comparison between the estimated and measured crack lengths for the R=-1 specimens, shown in Table 3, verifies the validity of the crack growth rates for these specimens. The reason for the higher apparent crack growth in the R=0.3 specimens is not completely understood and probably should be investigated further. The optically measured crack extensions obtained from the R=0.3 specimens, shown in Table 3, demonstrate that more crack growth occurred in these specimens than was estimated by the compliance method. This suggests that the crack growth rate was greater than that shown in Fig. 22. In most cases the L-R orientation appeared to demonstrate slightly slower crack growth rates than the L-C orientation.

COMBINED CYCLIC K AND J RESULTS

It was originally observed by Dowling and Begley[11] that cyclic K and J data can be combined on a single plot using the equation originally proposed by Rice[12] that:

$$K^2 = E' * J \qquad (8)$$

where,

$$E' = \frac{E}{1-\nu^2}, \qquad (9)$$

and,

E = material elastic modulus

ν = material Poisson's ratio

Such a plot for this material is shown in Fig. 23 and includes the high cycle ΔK results of the FCGR tests and the low cycle ΔJ results of the elastic-plastic tests. Also shown on Fig. 23 is a correlation equation for austenitic stainless steel from the standard textbook of Rolfe and Barsom,[4] and a set of Japanese[1] data from the HLVT program previously used to characterize this material. It was clear that in terms of J range the high and low cycle work done as a part of this study are consistent, and in close agreement with the standard textbook equation. The Japanese data differ by approximately one order of magnitude. The details of the methods used to obtain the Japanese data were not known except that the specimens were oriented in the L-C orientation and were of 1T scale. From our experience on this project it also appears that the Japanese data were obtained using a negative R ratio cyclic load history since this is the only way in which such large cyclic K or J ranges could be achieved. An attempt was made as a part of the project to simulate the Japanese data by re-analyzing our R=-1.0 data using another analysis and method to define the closure load. Since ΔJ (or ΔK) can only be increased by reducing the closure load, the first assumption was to use the minimum load for closure and to calculate ΔJ and then ΔK using the full area under each load cycle. The effect this had on a particular specimen is shown in Fig. 24. As expected the data was shifted to higher ΔK values at corresponding crack growth rates. A comparison of the adjusted data and the Japanese data is shown in Fig. 25. The correspondence is clearly excellent.

In an attempt to explain the rate of fatigue crack growth in the HLVT pipe elbow structure, the closure load at which the crack opens must be accurately determined. Clearly, complete closure of the fatigue crack occurred at load levels well above the minimum compressive load achieved in the laboratory specimen used in this investigation. Such closure would also be expected in the actual structure (pipe elbow) and could be more significant in the structure than in the laboratory specimen. The Japanese data from the HLVT program appears to have been generated by assuming that the entire loading range (maximum tensile load to minimum compressive load) contributed to the crack driving force. This has the net effect of lowering the overall crack growth rate for a given driving force (J-integral), as previously described. It is considered that this approach may not model the actual crack growth in the structure as well as applying laboratory data that has been properly adjusted for closure.

CONCLUSIONS

(1) The cast stainless steel is very resistant to ductile crack extension. J-resistance curves follow blunting behavior to very high J levels, well beyond the standard validity region defined by ASTM E1152.

(2) High cycle fatigue crack growth rate data obtained on the cast stainless steel is typical of that reported in standard textbooks.

(3) Low cycle fatigue crack growth rate data obtained for the cast stainless steel using the cyclic J integral approach is consistent with the high cycle fatigue crack growth rate and with the standard textbook correlation equation typical for this type of material.

(4) Evaluation of crack closure effects was essential to accurately determine the crack driving force for cyclic elastic-plastic crack growth in the cast stainless steel material.

RECOMMENDATIONS

Further FCGR tests with higher R ratios should be conducted to attempt to explain the observed elevation in crack growth rate for the R=0.3 tests conducted for this investigation. Fractography should also be performed on these specimens to evaluate the microfracture mode(s).

REFERENCES

[1] Park, Y.J., Cuerri, J.R., and Hofmayer, C.H., "The High Level Vibration Test Program Final Report," USNRC NUREG/CR-5585, 1991, U.S. Nuclear Regulatory Commission, Washington, D.C. 20555

[2] The Metals Handbook, Ninth Edition, Vol. 15, CASTINGS, American Society for Metals, pp. 296-307, 1988

[3] Joyce, J.A. and Gudas J.P., "Computer Interactive J_{Ic} Testing of Navy Alloys," Elastic-Plastic Fracture, ASTM STP 668, American Society for Testing and Materials, Philadelphia, PA, 1979, pp. 451-468.

[4] Rolfe, S.T. and Barsom, J.M., Fracture and Fatigue Control in Structures, Prentice-Hall, Inc., Englewood Cliffs, New Jersey, 1977.

[5] Tanaka, I., Hoshide, I. and Nakata, M., "Elastic-Plastic Crack Propagation Under High Cyclic Stresses," Elastic-Plastic Fracture: Second Symposium, ASTM STP 803, American Society for Testing and Materials, Philadelphia, PA, 1983, pp. II 708-722.

[6] El Haddad, M.H. and Murkherjee, B., "Elastic-Plastic Fracture Mechanics Analysis of Fatigue Crack Growth,"Elastic-Plastic Fracture: Second Symposium, ASTM STP 803, American Society for Testing and Materials, Philadelphia, PA, 1983, pp. II 689-707.

[7] Joyce, J.A. and Sutton, G.E., "An Automated Method of Computer Controlled Fatigue Crack Growth Testing Using the Elastic-Plastic Parameter Cyclic J," Automated Method of Computer Controlled Low-Cycle Fatigue Crack Growth, ASTM STP 877, American Society for Testing and Materials, Philadelphia, PA, 1985, pp. 227-247.

[8] Joyce, J.A., "Characterization of the Effects of Large Unloading Cycles on Ductile Tearing Toughness of HSLA Steel," Journal of Testing and Evaluation, Vol. 18, No. 6, Nov. 1990, pp. 373-384.

[9] Merkle, J.G. and Corten, H.T., "A J-Integral Analysis for the Compact Specimen Considering Axial Forces as well as Bending Effects," Journal of Pressure Vessel Technology, Transaction of ASME, 1974, pp. 286-292.

[10] Clarke, G.A. and Landes, J.D., "Evaluation of J for the Compact Specimen," Journal of Testing and Evaluation, Vol. 7, No. 5., 1979, pp. 264-269.

[11] Dowling, N.E. and Begley, J.A., "Fatigue Crack Growth During Gross Plasticity and the J-Integral," Mechanics of Crack Growth, ASTM STP 590, American Society for Testing and Materials, Philadelphia, PA, 1976, pp. 82-103.

[12] Rice, J.R., Paris, P.C., and Merkle, J.G., "Some Further Results on J-Integral Analysis and Estimates," Progress in Flaw Growth and Fracture Toughness Testing, ASTM STP 536, American Society for Testing and Materials, 1973, pp. 231-245.

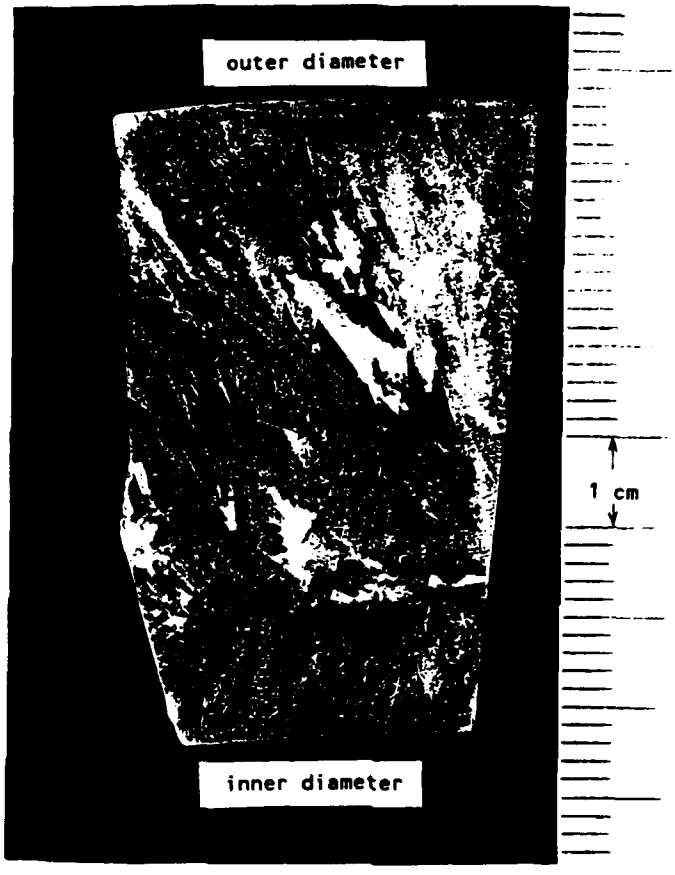

Fig. 1. Macroetch of Section Through Cast Stainless Steel HLVT pipe elbow

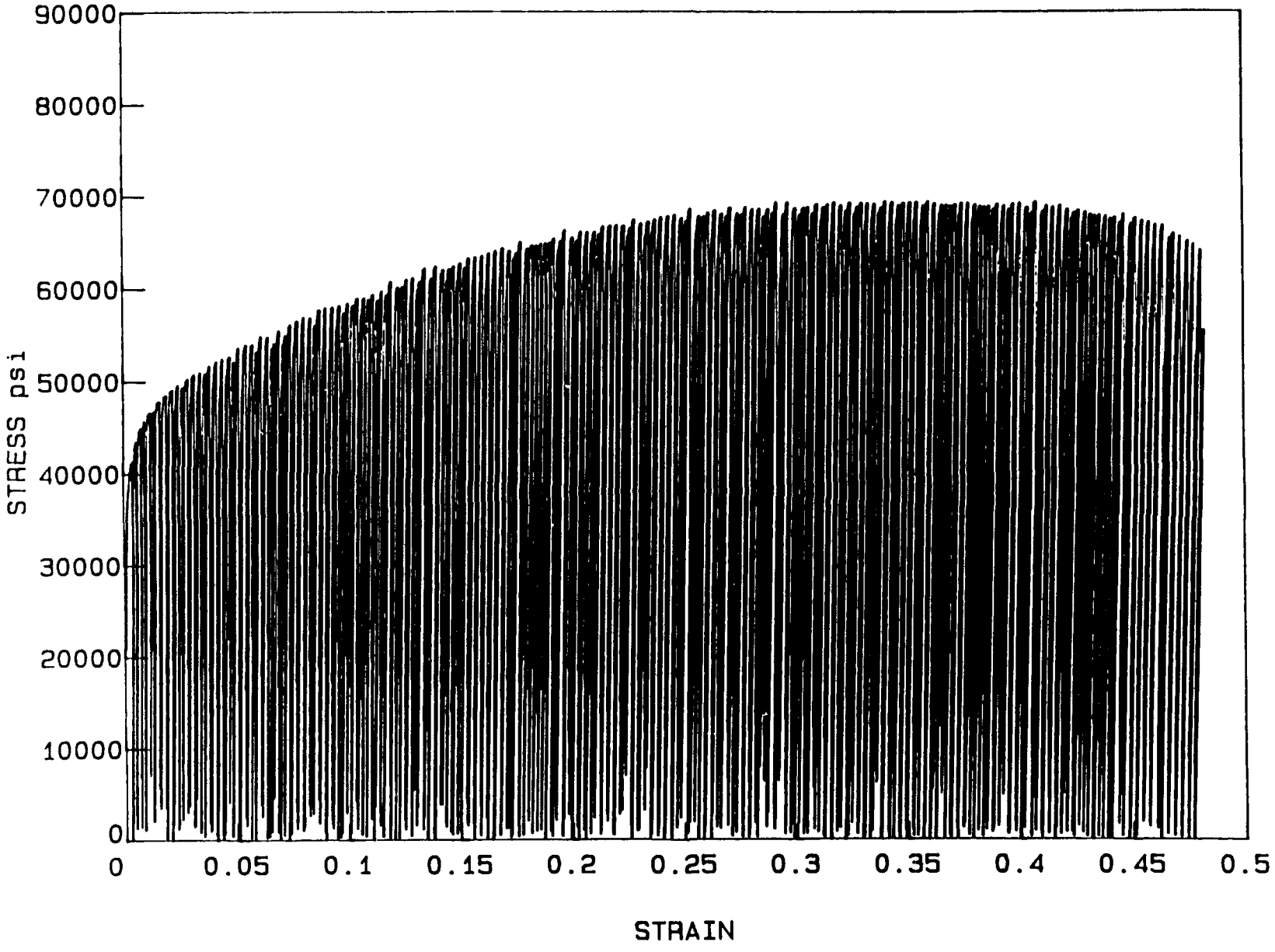

Fig. 2. Cyclic Tensile Stress-Strain Curve for Cast Stainless Steel Specimen GPQ-36

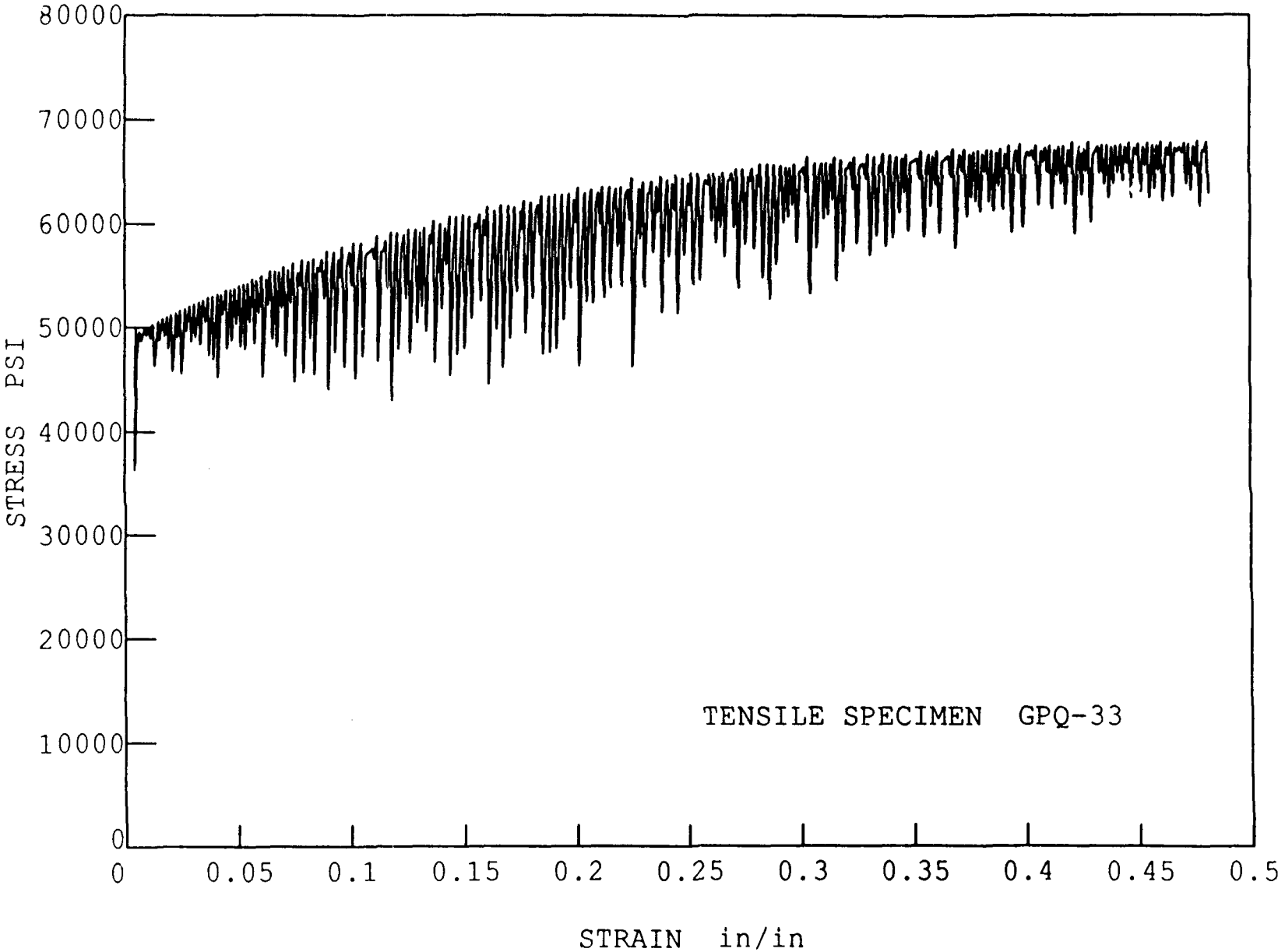

Fig. 3. Cyclic Tensile Stress-Strain Envelope for Cast Stainless Steel Specimen GPQ-33

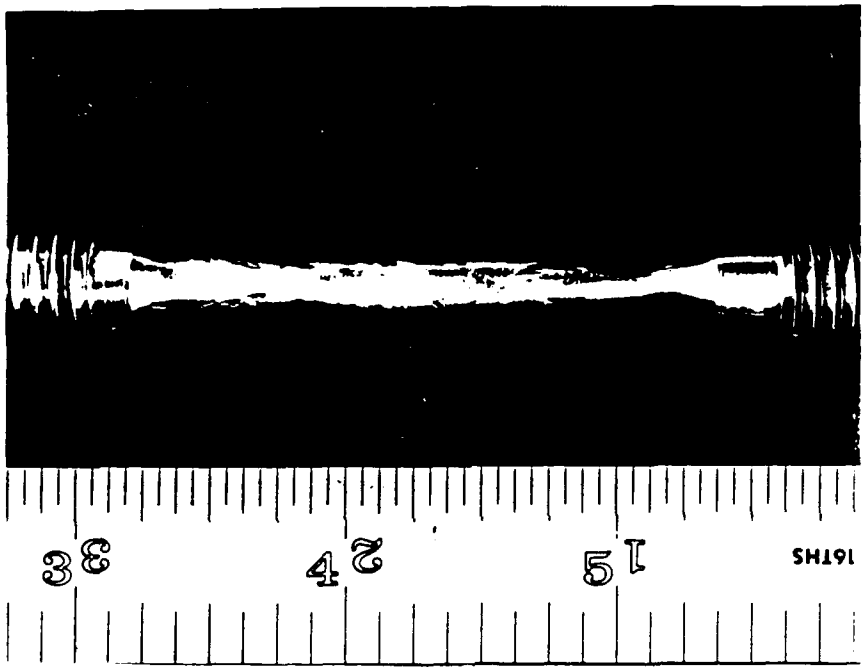

Fig. 4. Tensile Specimen of Cast Stainless Steel Showing Anisotropic Deformation

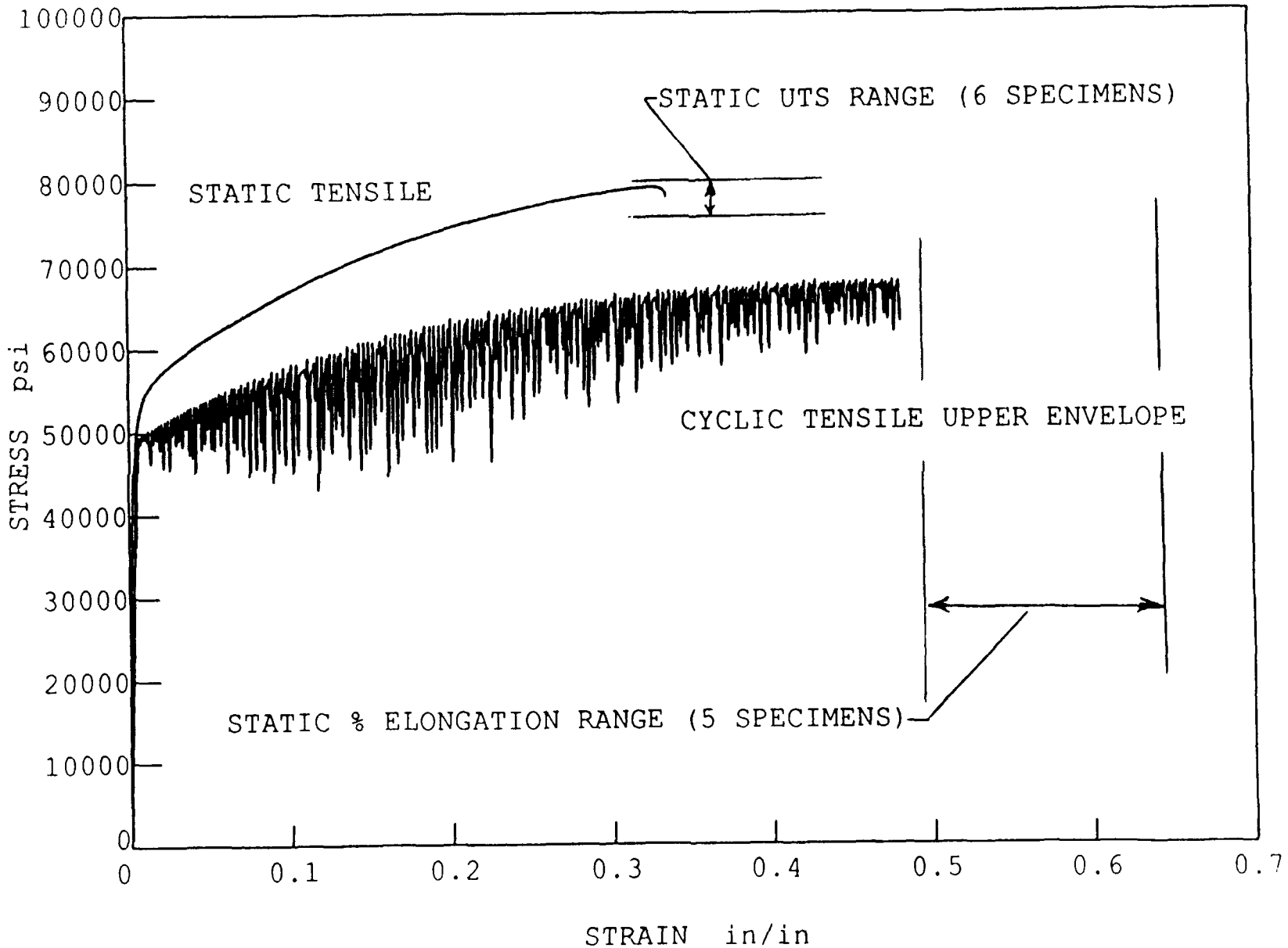

Fig. 5. Cyclic Tensile Stress-Strain Envelope and Static Tensile Stress-Strain Envelope for Cast Stainless Steel

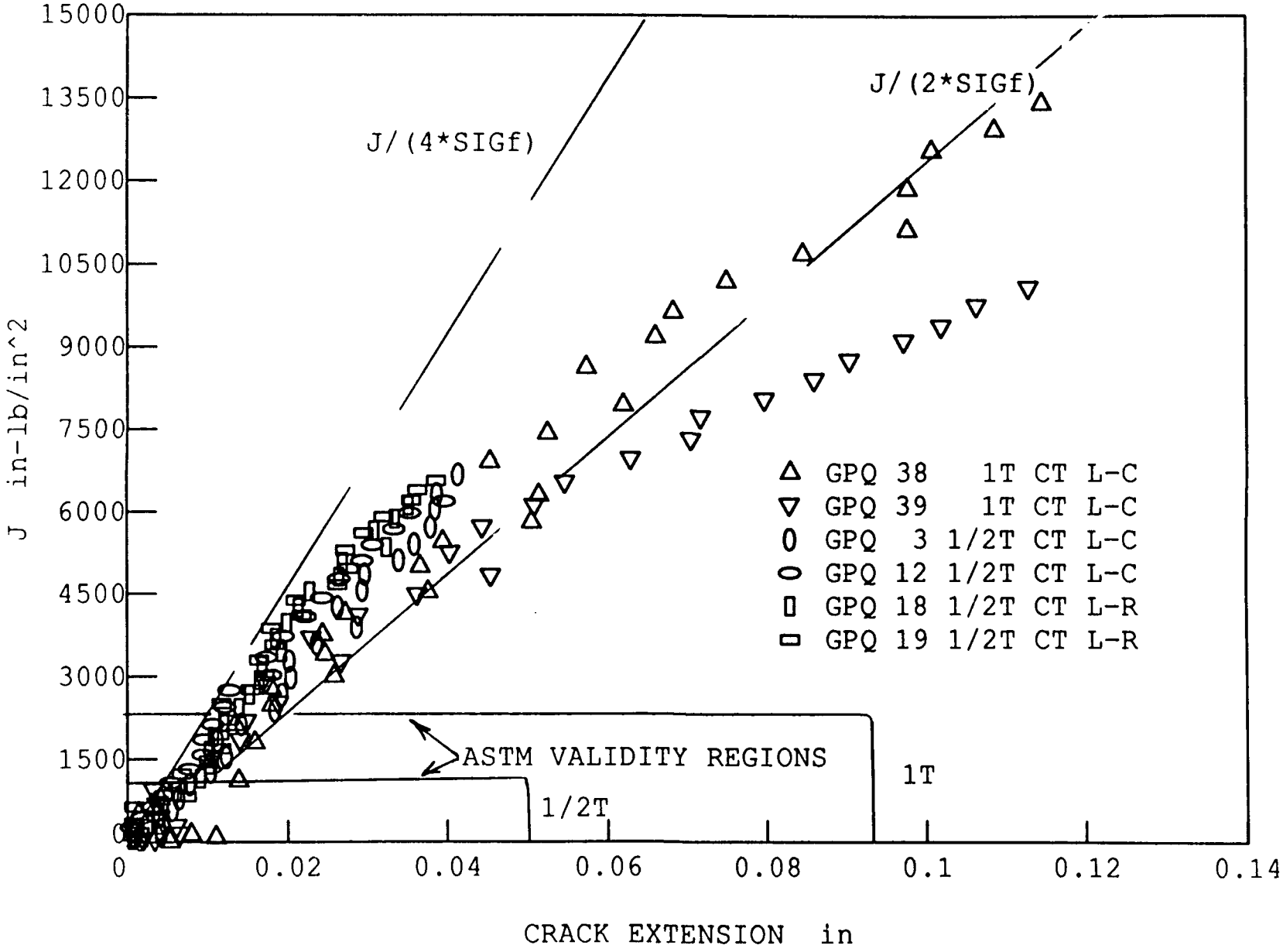

Fig. 6. Monotonic J-R curves for Cast Stainless Steel

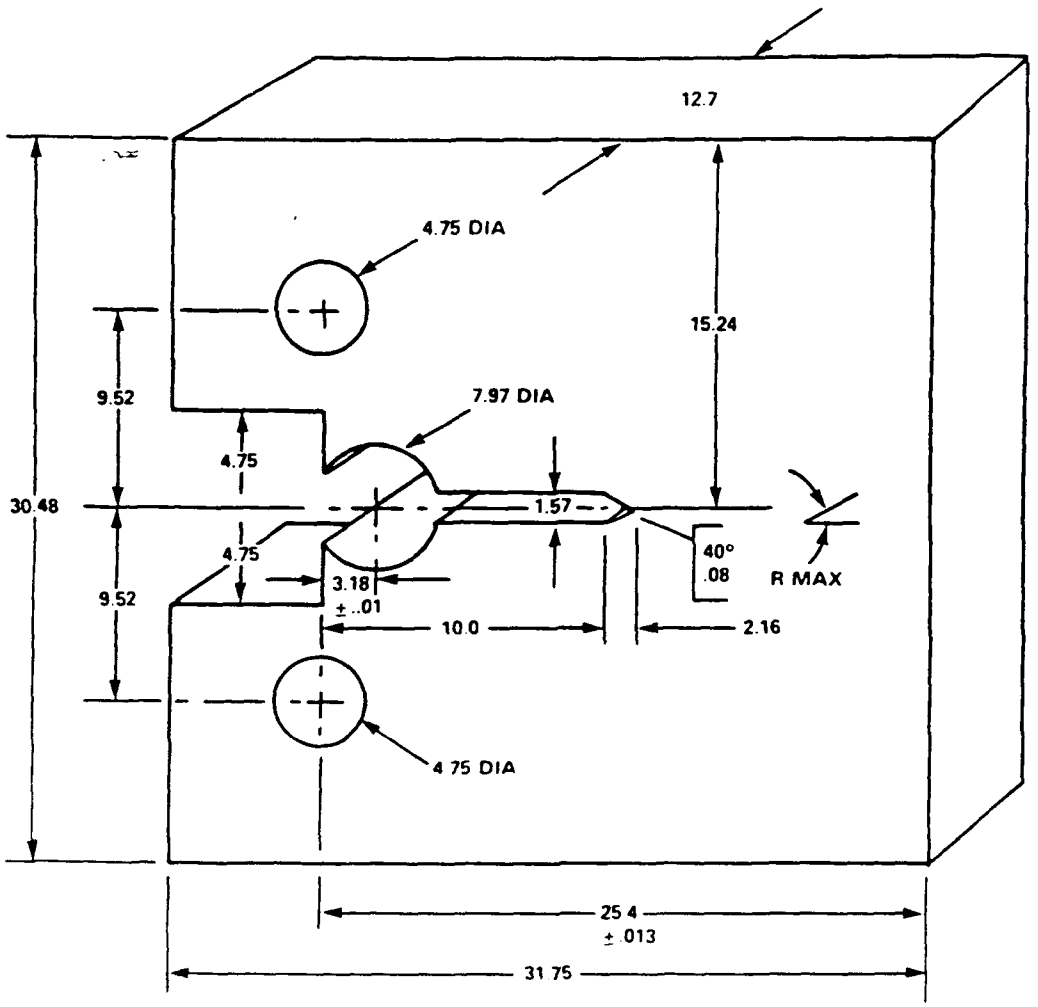

Fig. 7. 1/2T C(T) Specimen with Integral Knife Edges

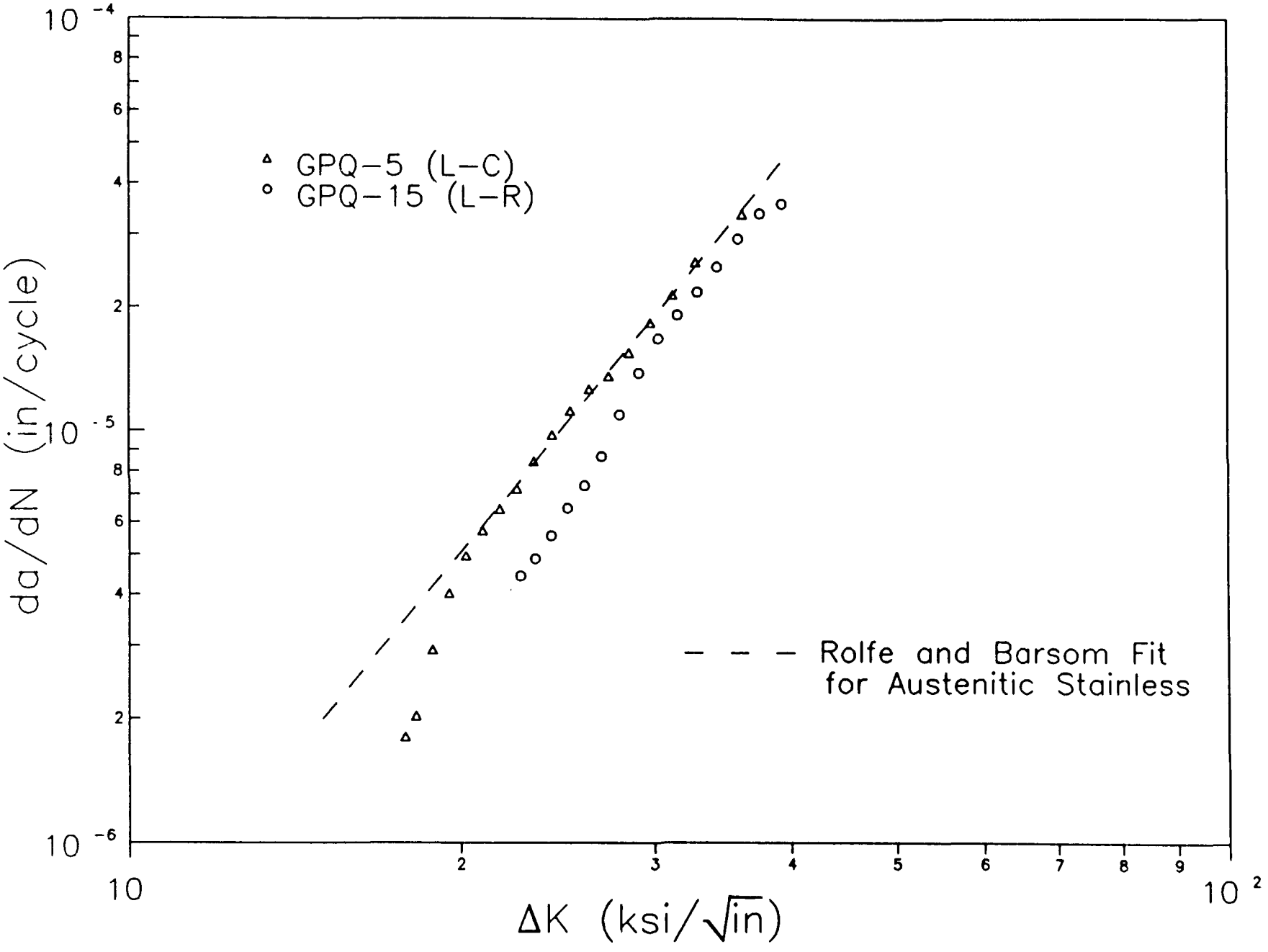

Fig. 8. High Cycle Fatigue Crack Growth Data for Cast Stainless Steel Showing Comparison with Rolfe and Barsom Fit

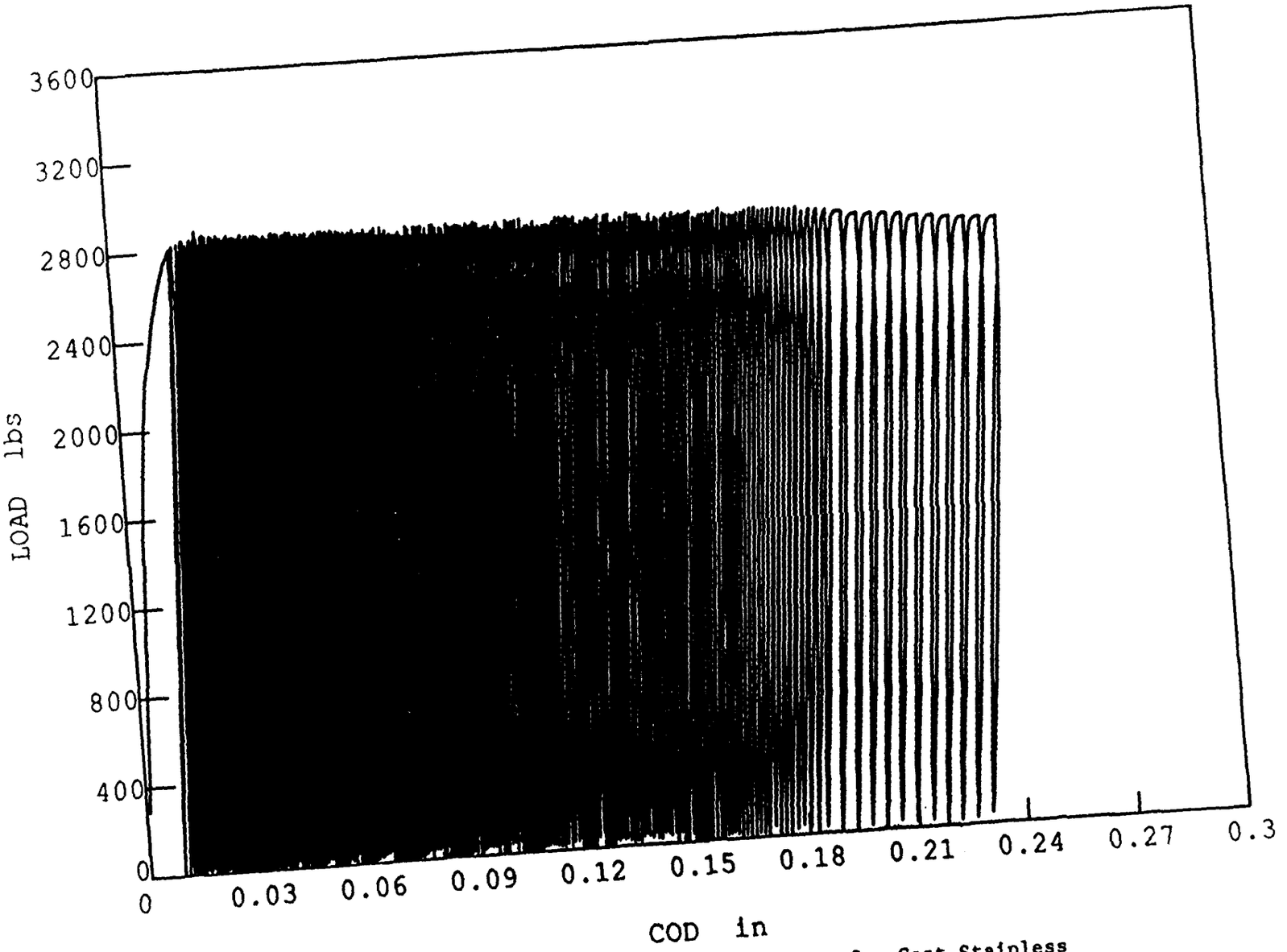

Fig. 9. Cyclic Load vs. Displacement Curve for Cast Stainless Steel, R=0 Specimen GPQ-11

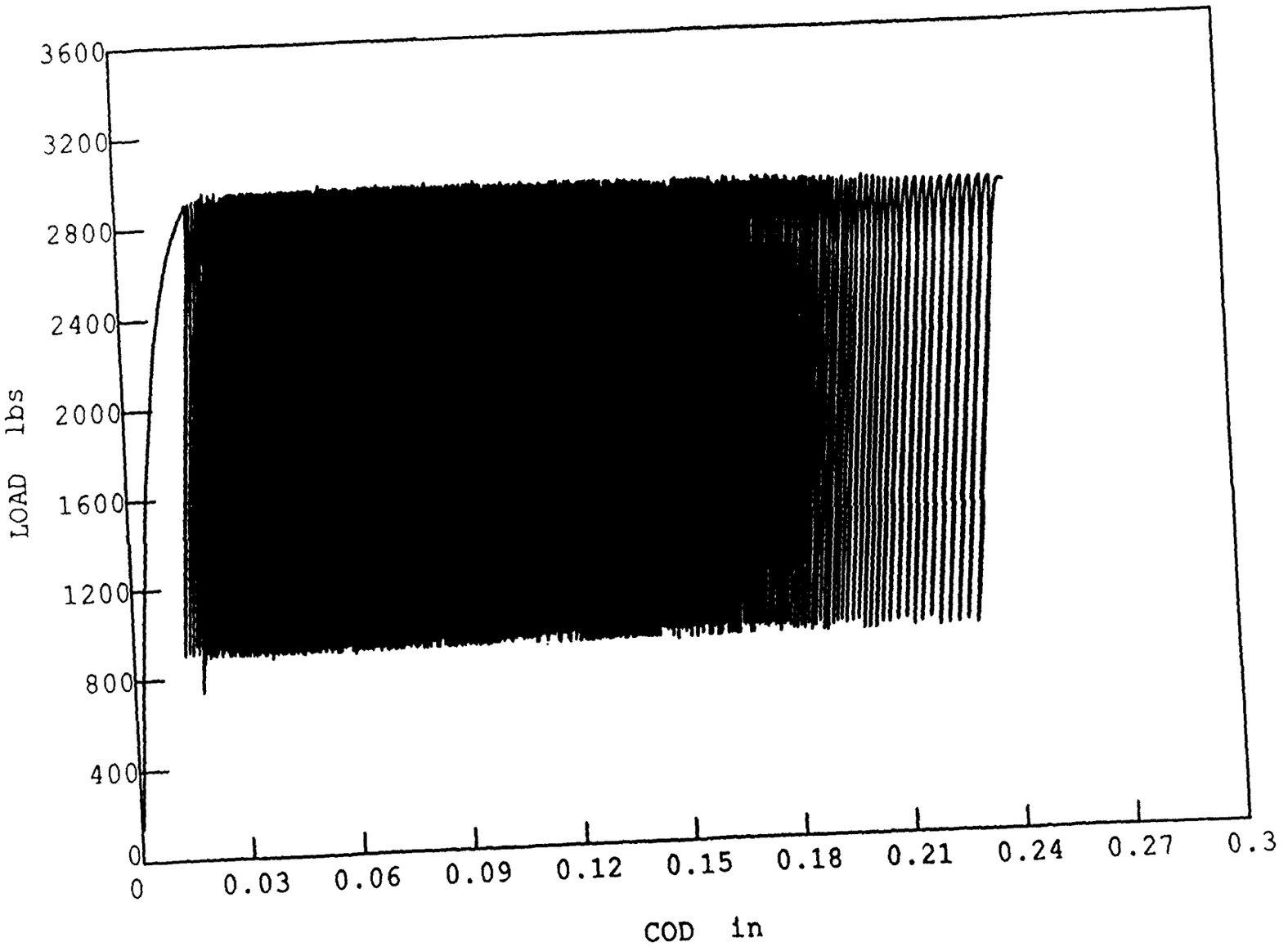

Fig. 10. Cyclic Load vs. Displacement Curve for Cast Stainless Steel, R=0.3 Specimen GPQ-20

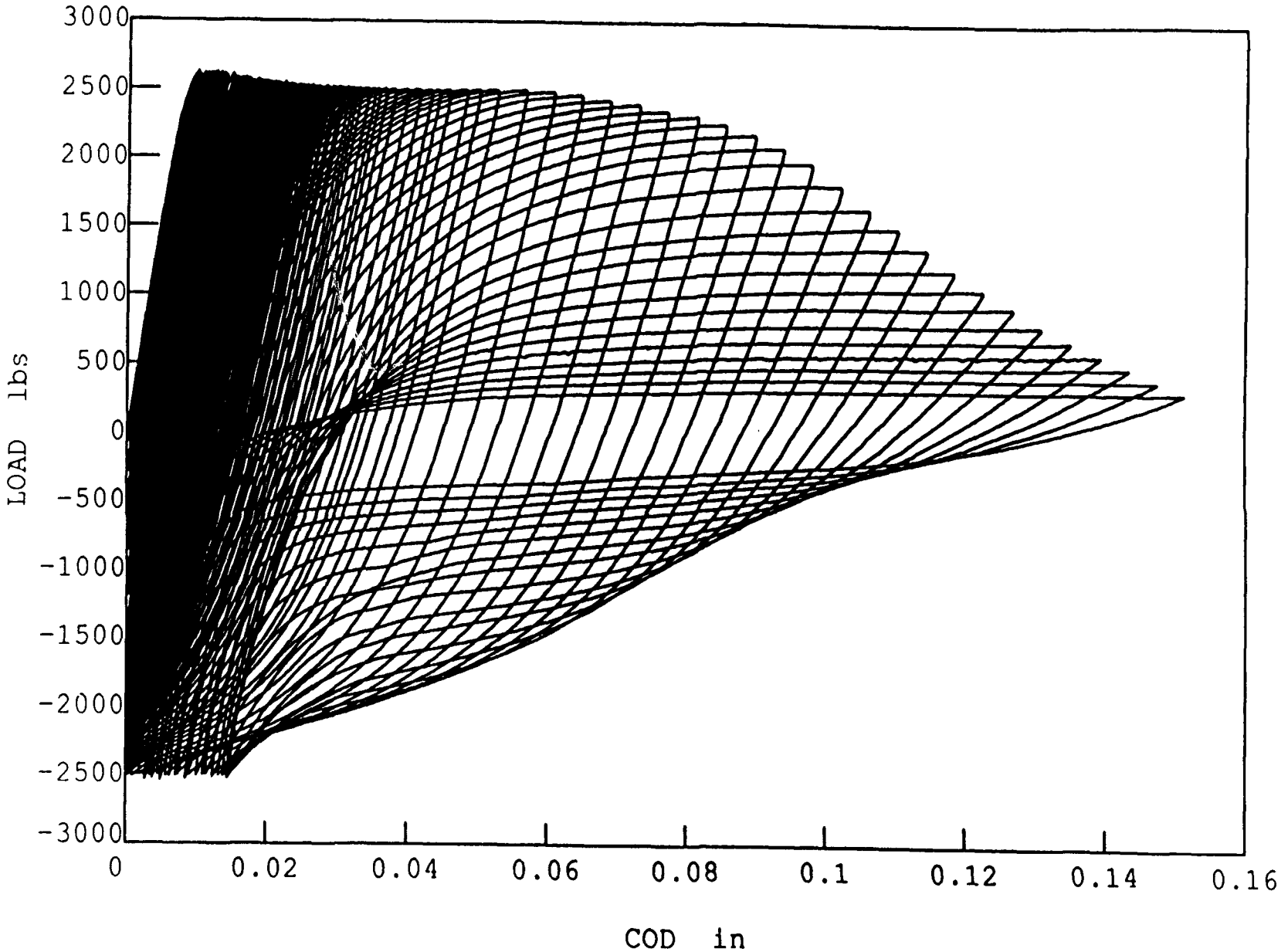

Fig. 11. Cyclic Load vs. Displacement Curve for Cast Stainless Steel, R=-1 Specimen GPQ-16

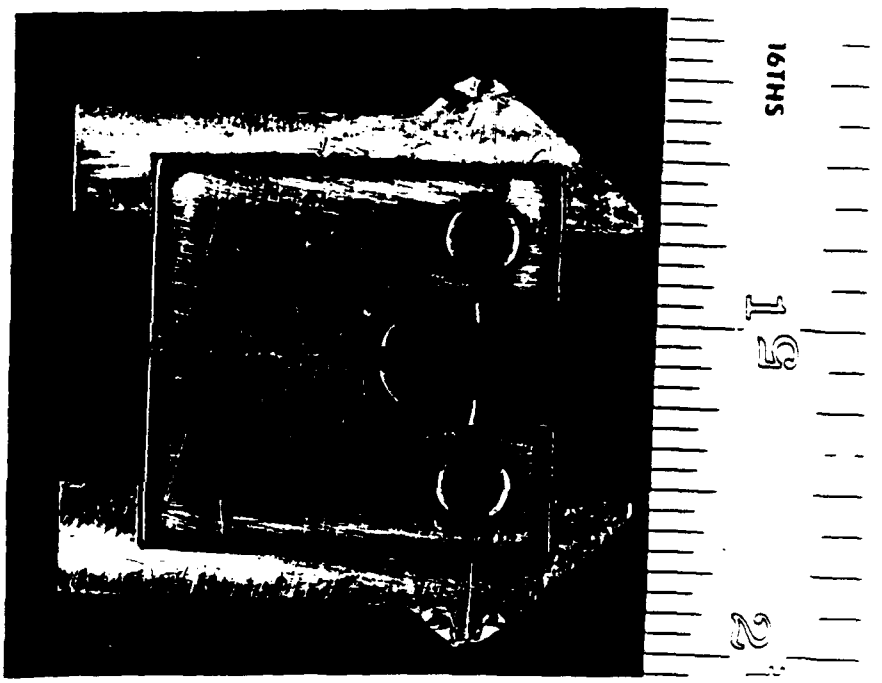

Fig. 12. Improved Load Cap Fixtures for 1/2T C(T) Specimens

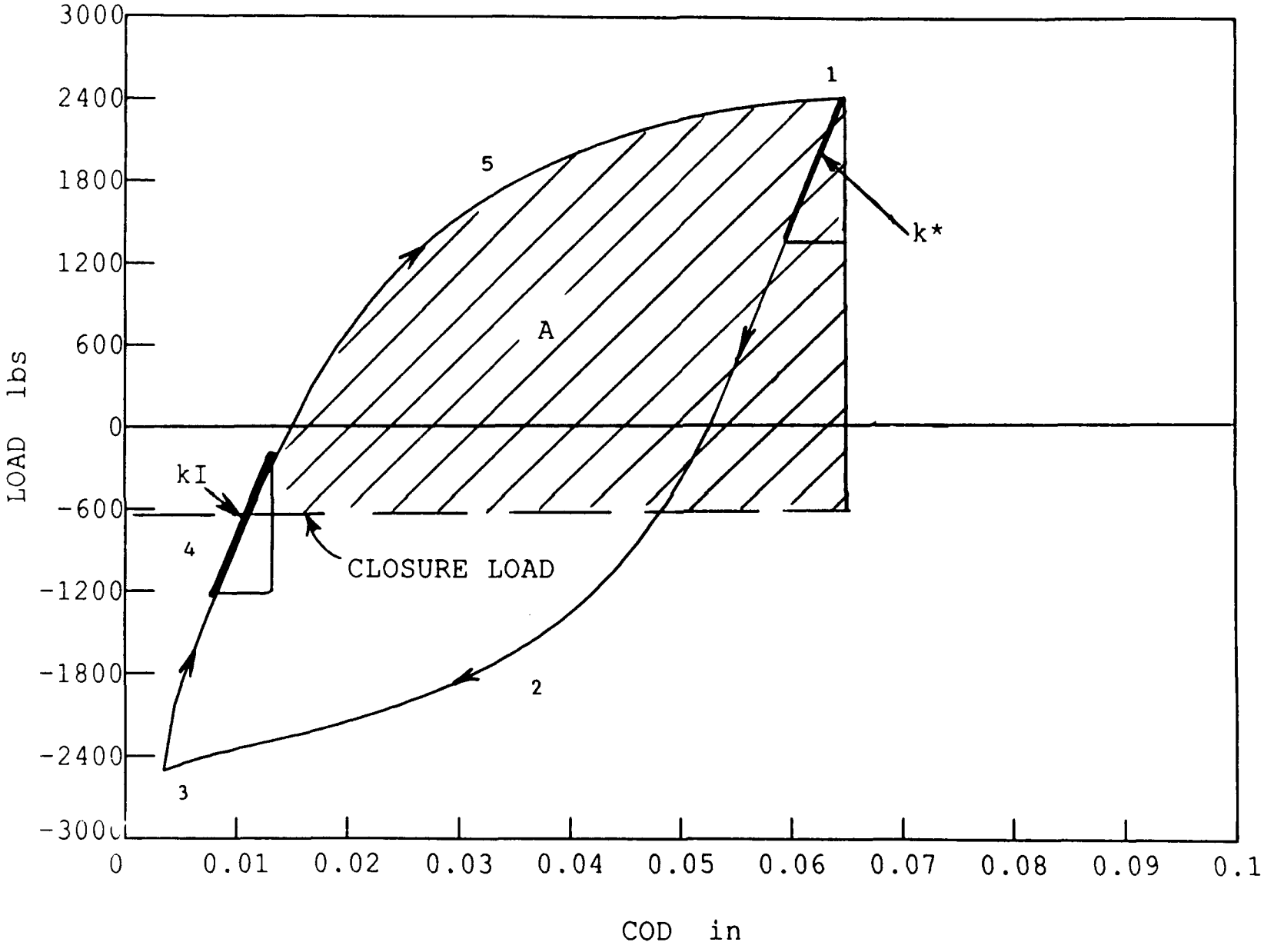

Fig. 13. Schematic of DTRC/USNA Analysis for Closure Load Calculation

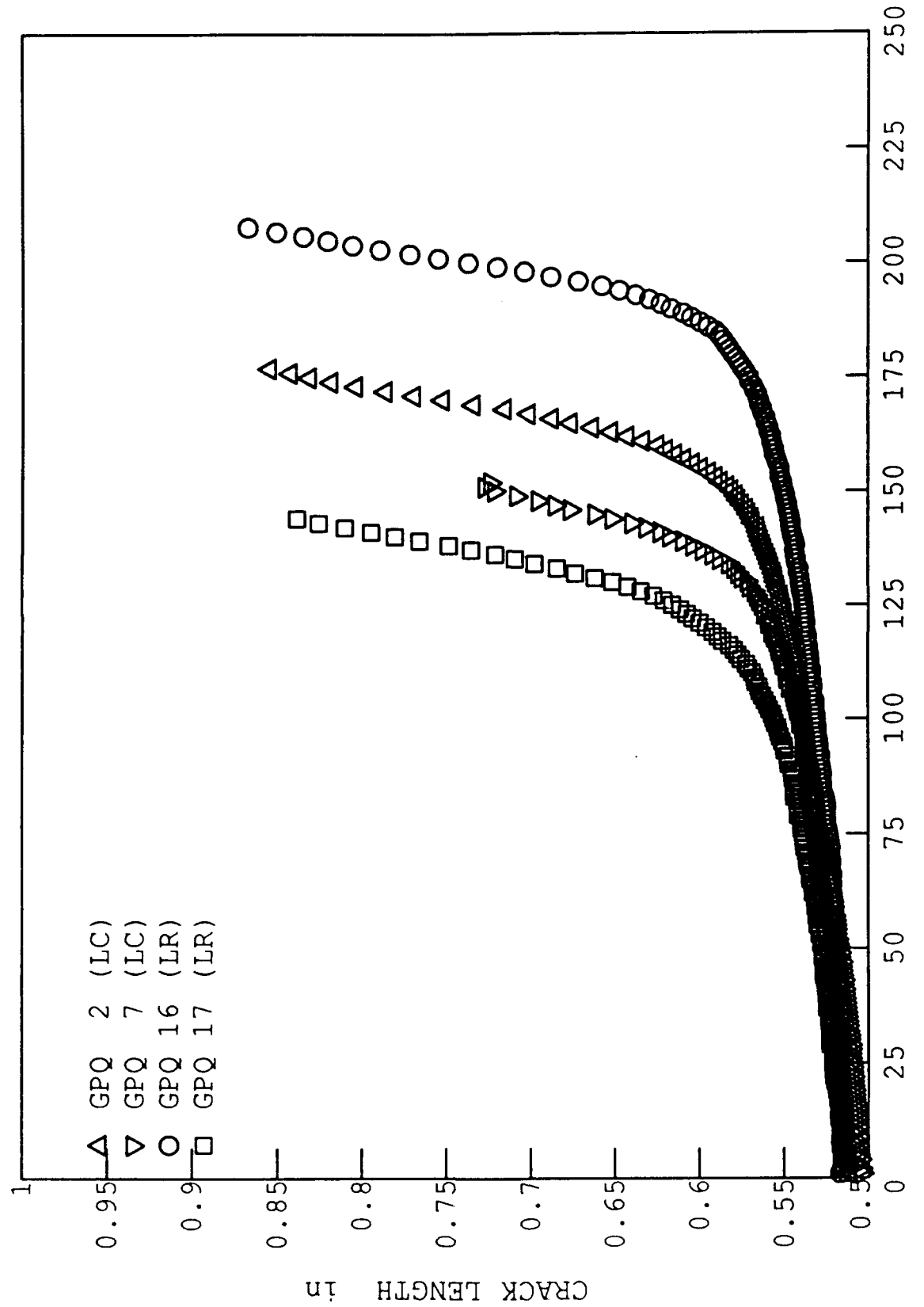

Fig. 14. Crack Length vs. Cycle Count for Cast Stainless Steel R=-1 Specimens

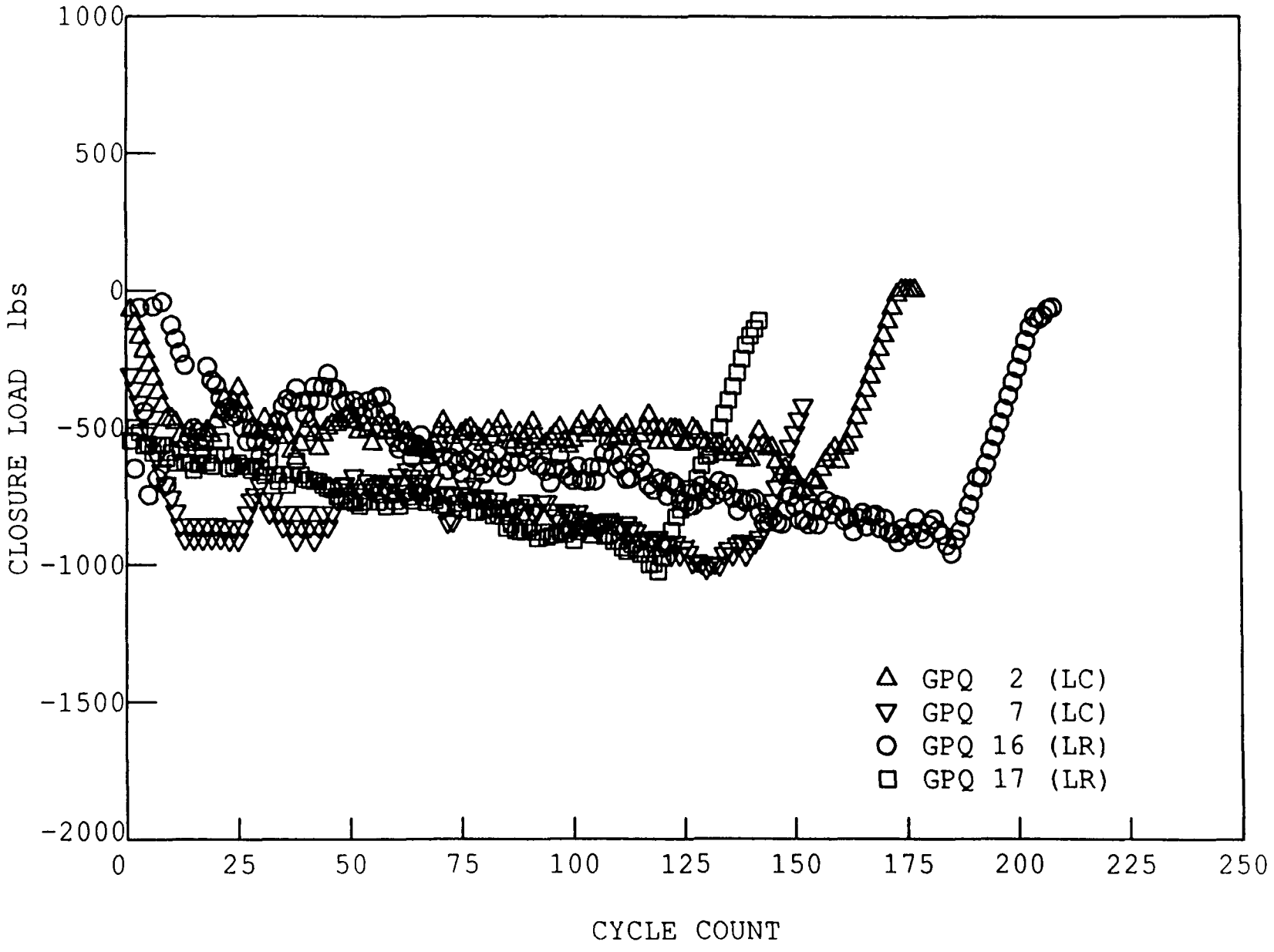

Fig. 15. Closure Load vs. Cycle Count for Cast Stainless Steel R=-1 Specimens

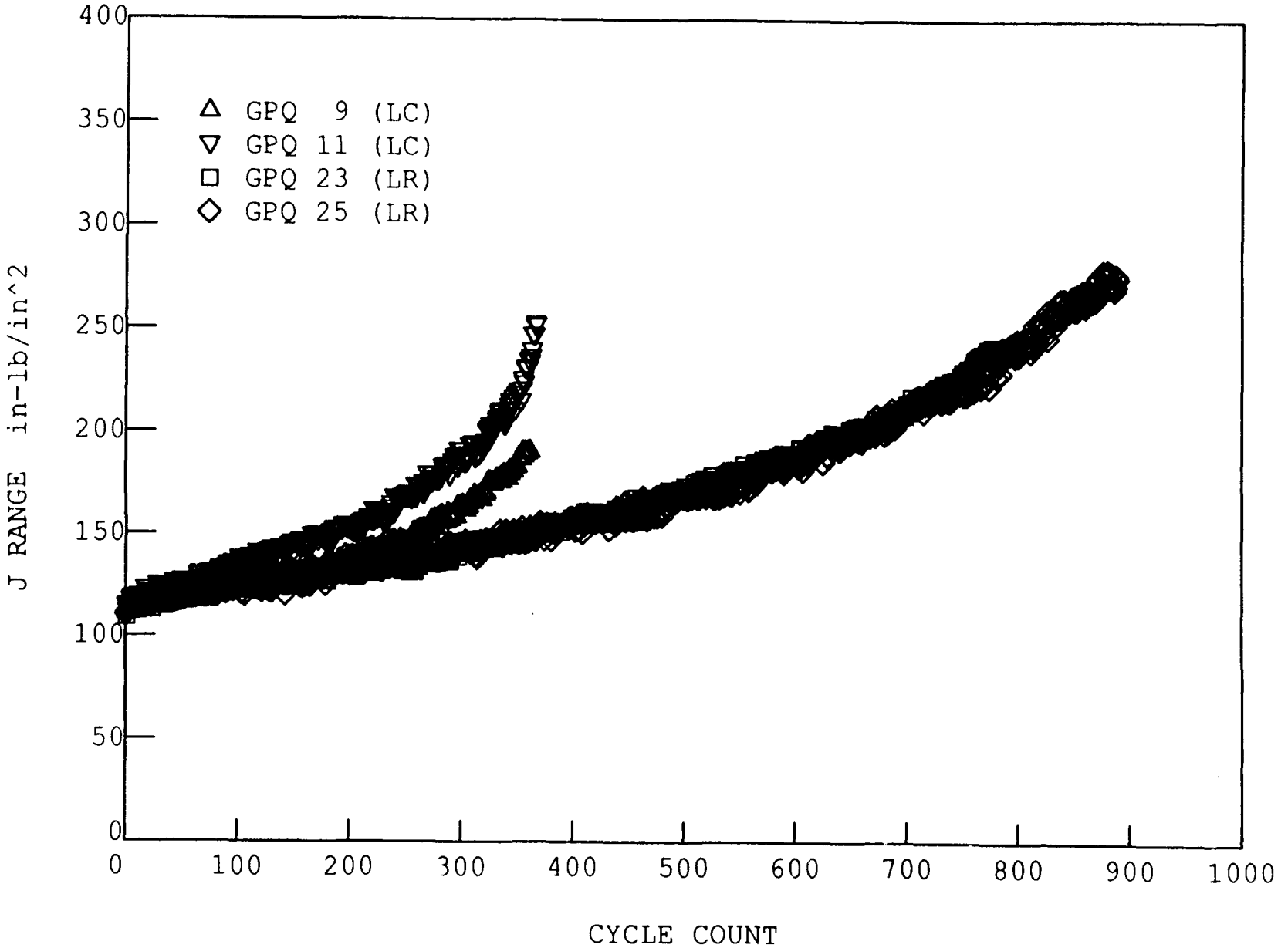

Fig. 16. J Range vs. Cycle Count for Cast Stainless Steel R-0 Specimens

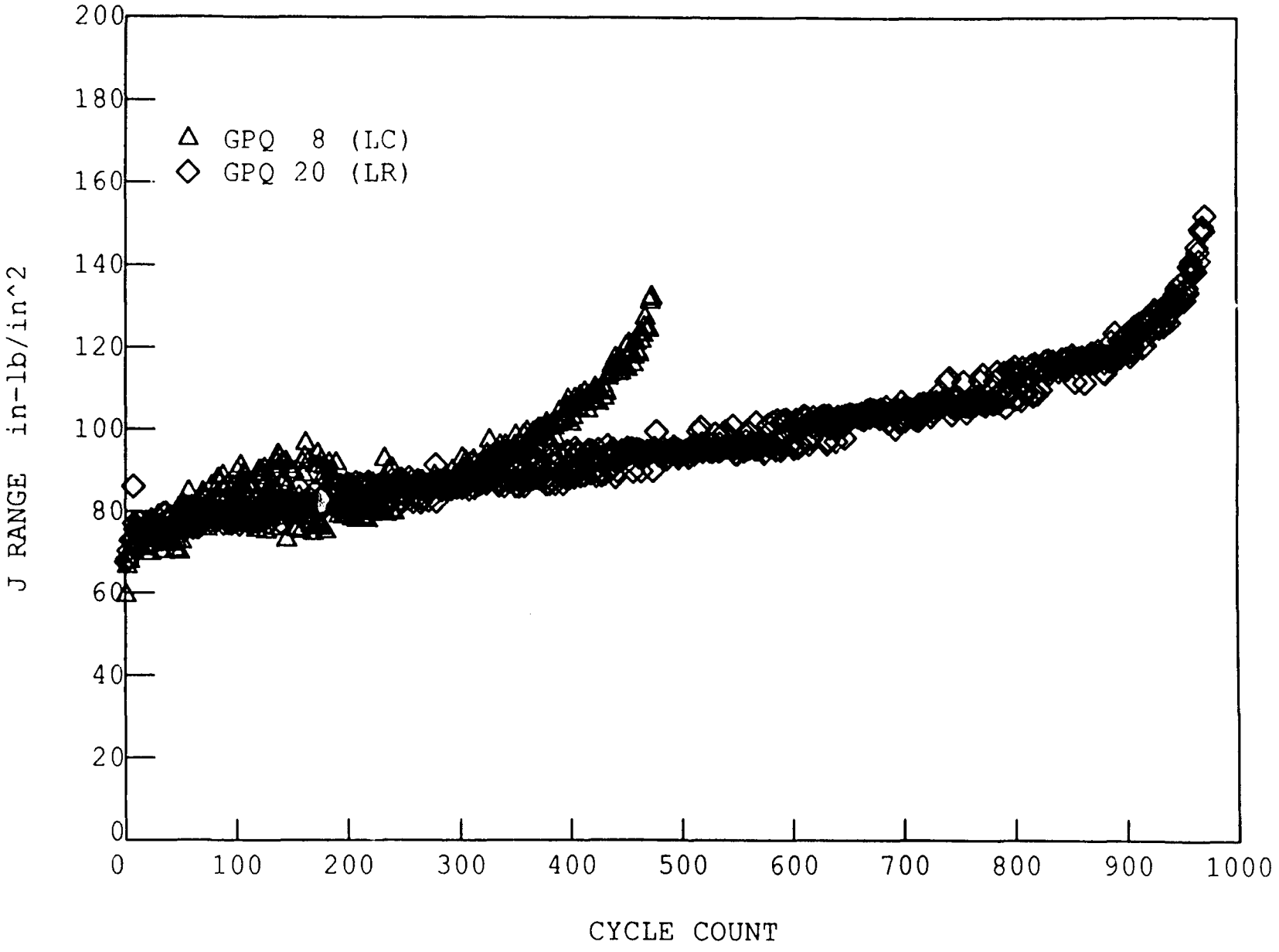

Fig. 17. J Range vs. Cycle Count for Cast Stainless Steel R-0.3 Specimens

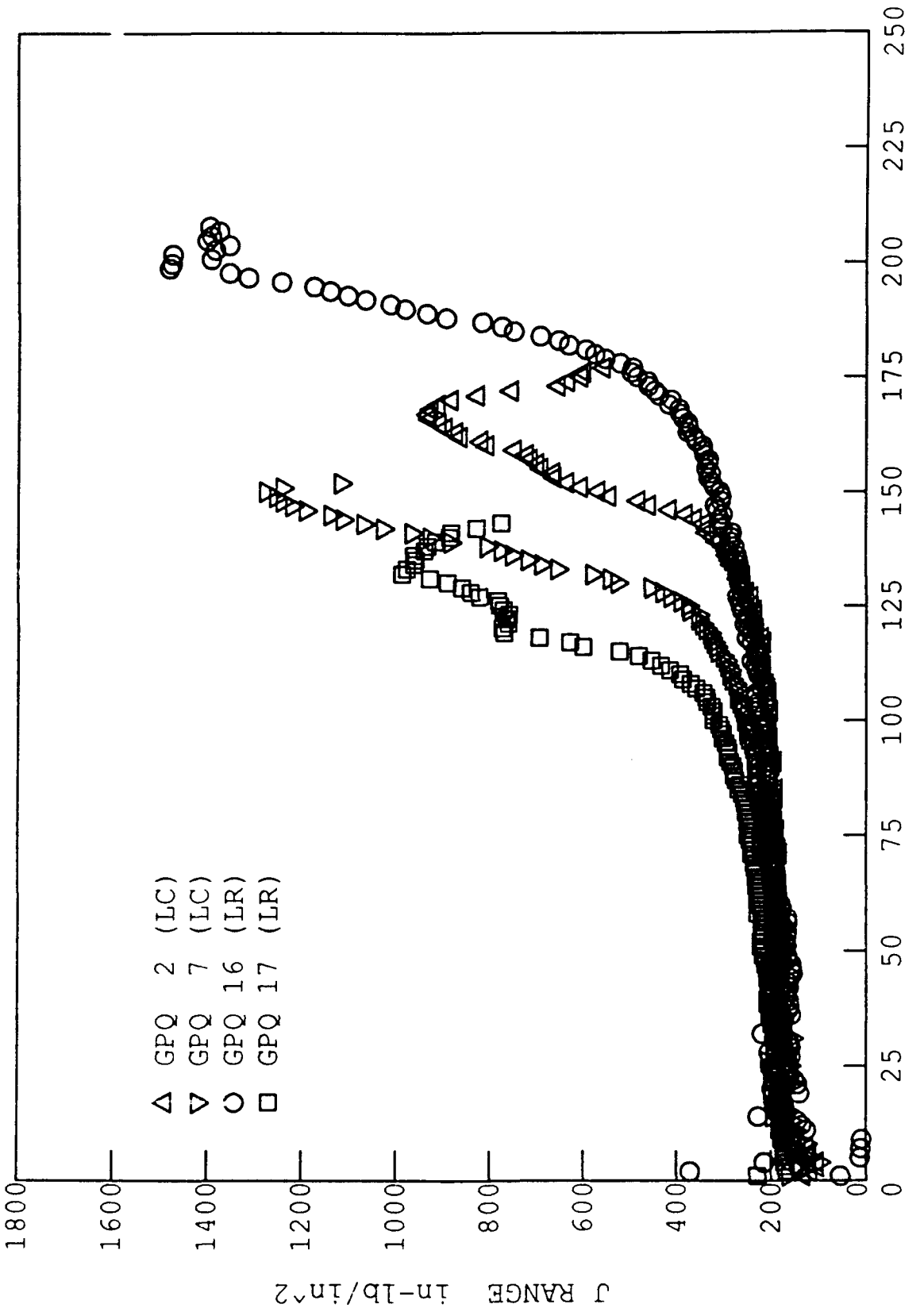

Fig. 18. J Range vs. Cycle Count for Cast Stainless Steel R=-1 Specimens

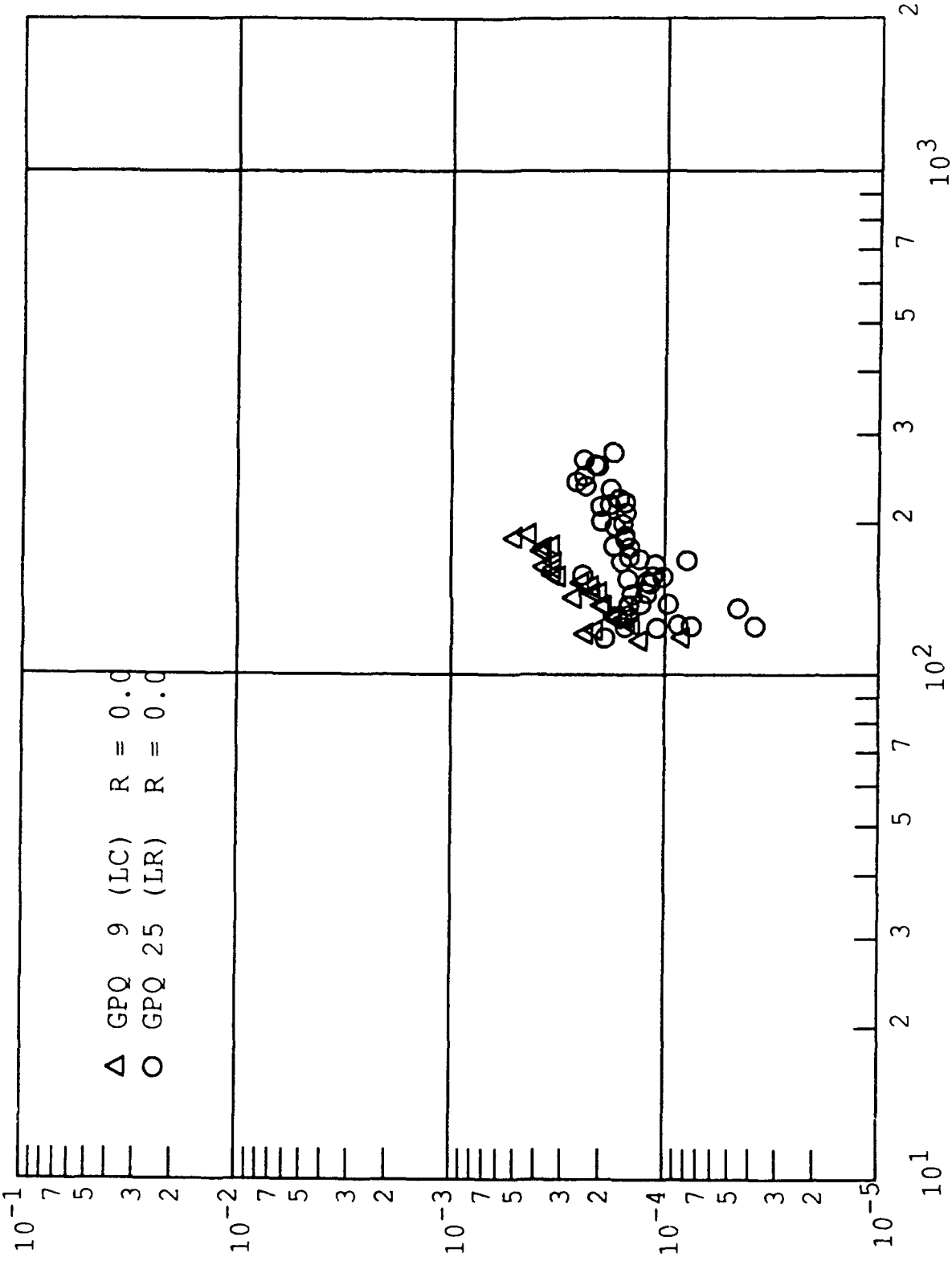

Fig. 19. Crack Growth Rate for Cast Stainless Steel R=0 Specimens

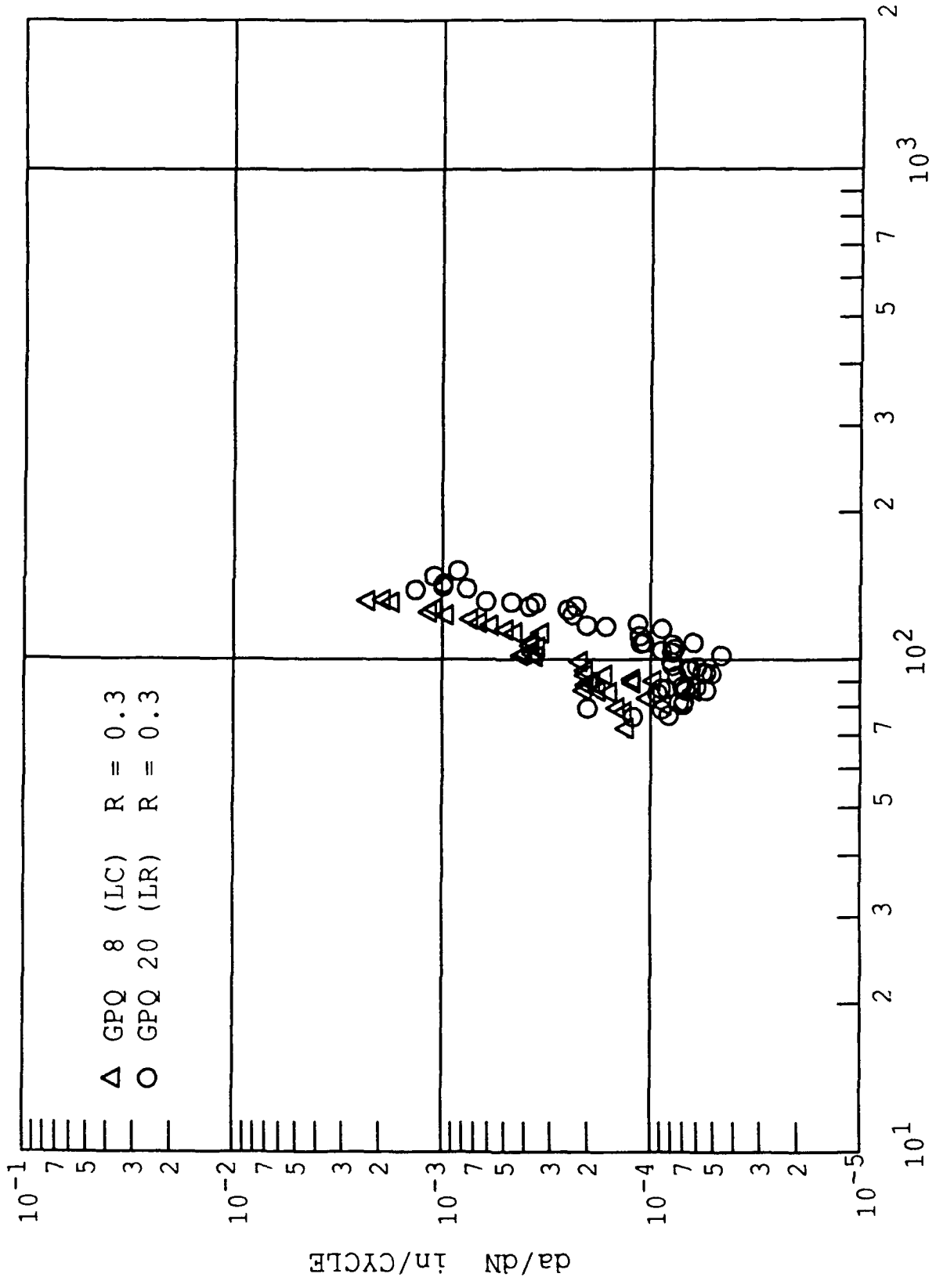

Fig. 20. Crack Growth Rate for Cast Stainless Steel R=0.3 Specimens

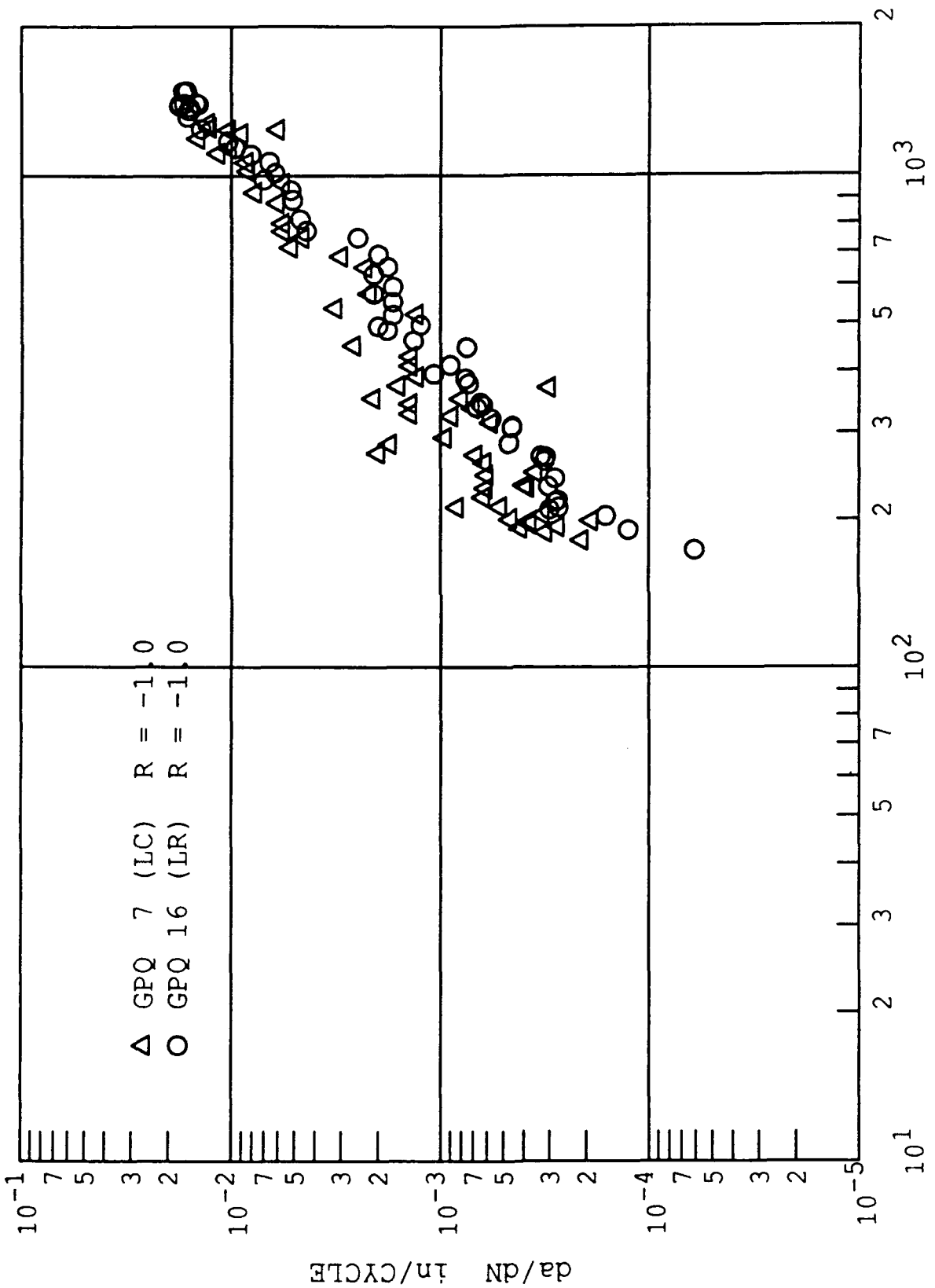

Fig. 21. Crack Growth Rate for Cast Stainless Steel R=-1 Specimens

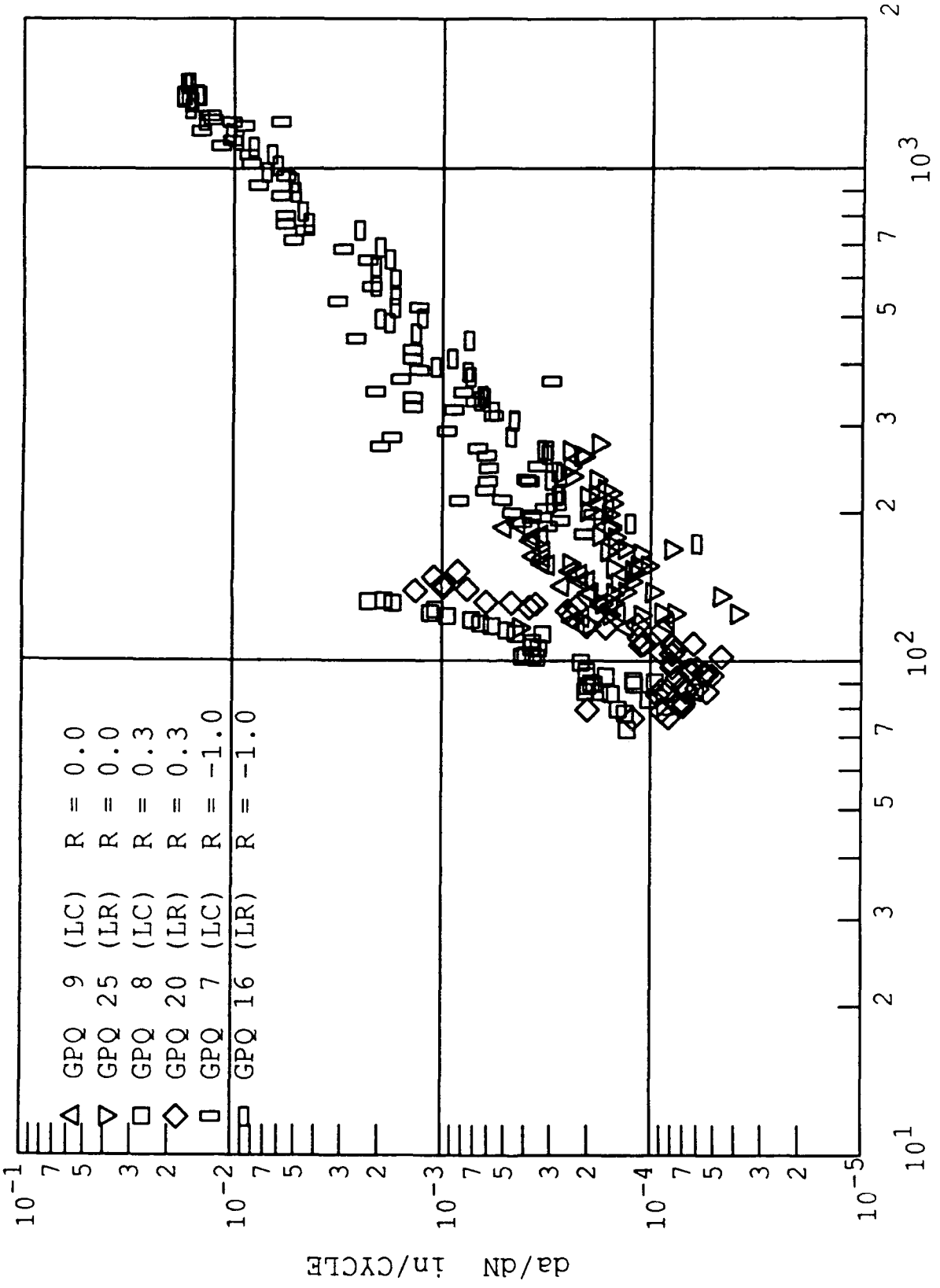

Fig. 22. Crack Growth Rate for Cast Stainless Steel (Combined R Ratios)

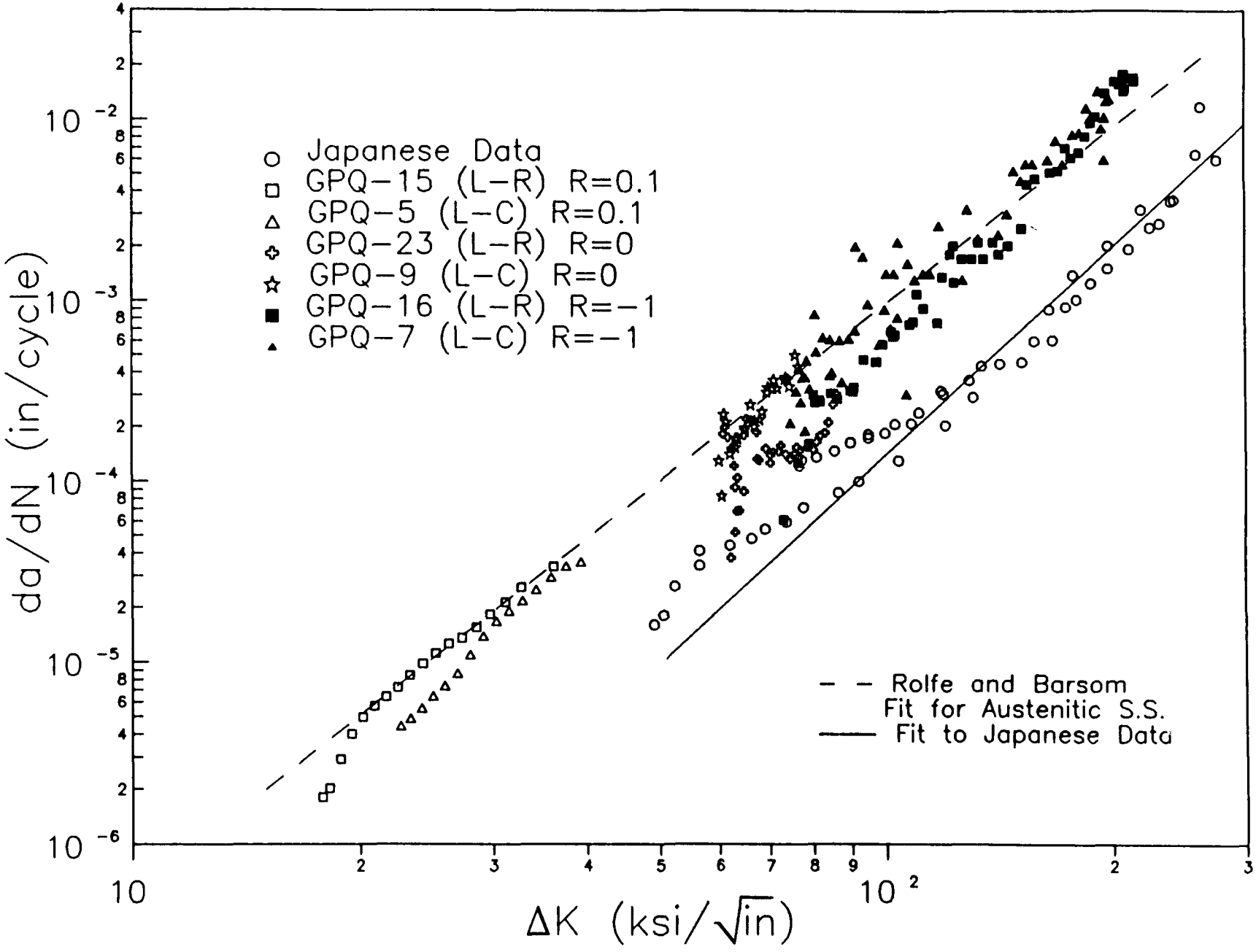

Fig. 23. Comparison of Japanese and DTRC/USNA Crack Growth Rates for Cast Stainless Steel

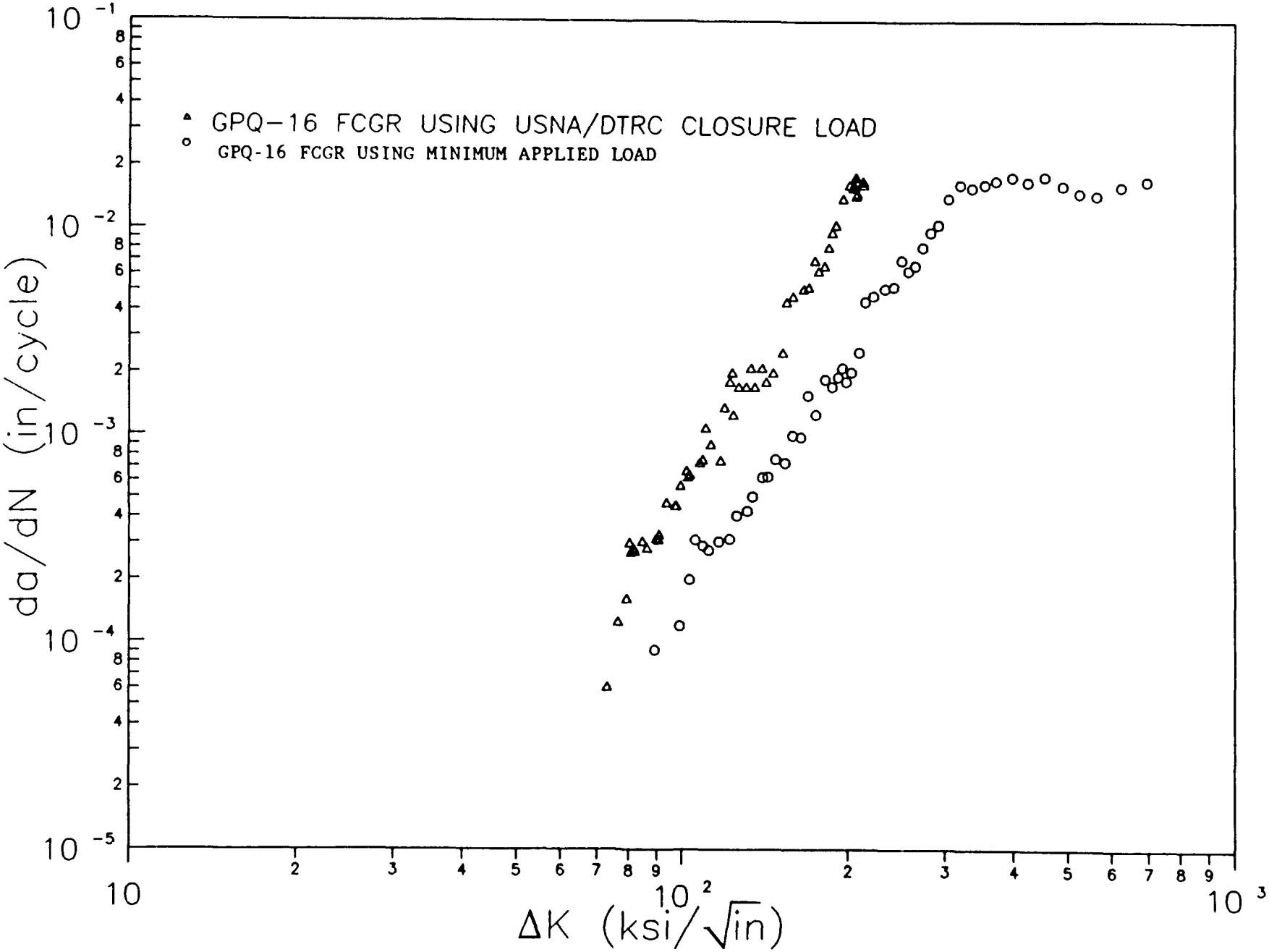

Fig. 24. DTRC/USNA Crack Growth Rates for Cast Stainless Steel with Different Closure Loads

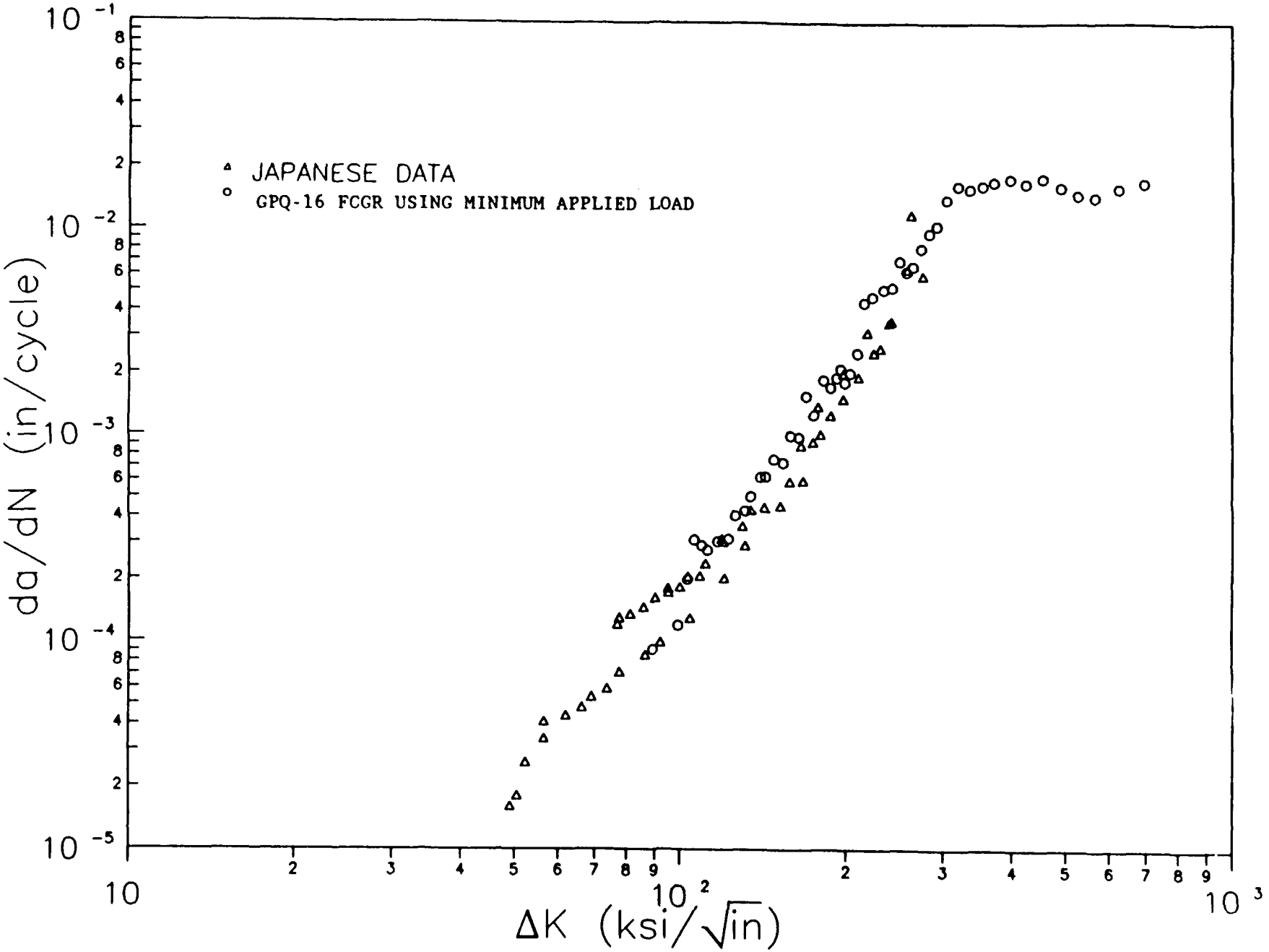

Fig. 25. DTRC/USNA Crack Growth Rate for Cast Stainless Steel at Minimum Closure Load Compared with Japanese Crack Growth Rate Data

INITIAL DISTRIBUTION

OUTSIDE CENTER

Copies

4 U.S. Nuclear Regulatory Commission
Division of Engineering
Materials Engineering Branch
Mail Stop 007NL
Washington, D.C. 20555
Attn: M. Mayfield/A. Hiser

12 DTIC

CENTER DISTRIBUTION

1	011.5	Caplan
1	28	Wacker
1	2801	Crisci
1	2803	Cavallaro
1	2803	Hardy
1	2809	Malec
1	281	Holsberg
1	281.S	Cropley
4	2814	Montemarano
10	2814	Hackett
5	2814	Roe
1	2813	Ferarra
1	2812	Moran
1	2815	DeNale
1	283	Singerman
1	284	Fischer
1	522.1	TIC
1	5231	Office Services

REPORT DOCUMENTATION PAGE

Form Approved
OMB No. 0704-0188

1. AGENCY USE ONLY *(Leave blank)*	2. REPORT DATE	3. REPORT TYPE AND DATES COVERED
	October 1991	Research & Development

4. TITLE AND SUBTITLE
Effects of Cyclic Loading on the Deformation and Elastic-Plastic Fracture Behavior of a Cast Stainless Steel

5. FUNDING NUMBERS

6. AUTHOR(S)
J.A. Joyce, E.M. Hackett, and C. Roe

7. PERFORMING ORGANIZATION NAME(S) AND ADDRESS(ES)
David Taylor Research Center
Code 2814
Annapolis MD 21402

8. PERFORMING ORGANIZATION REPORT NUMBER
DTRC/SME-91-11

9. SPONSORING /MONITORING AGENCY NAME(S) AND ADDRESS(ES)
U.S. Nuclear Regulatory Commission
Division of Engineering
Washington DC 20555
Attn: Mr. Mr. Mayfield/Mr. A. Hiser

10. SPONSORING /MONITORING AGENCY REPORT NUMBER

11. SUPPLEMENTARY NOTES

12a. DISTRIBUTION / AVAILABILITY STATEMENT
Approved for public release; distribution is unlimited.

12b. DISTRIBUTION CODE

13. ABSTRACT *(Maximum 200 words)*

Tests conducted in Japan as part of the High Level Vibration Test (HLVT) program for reactor piping systems revealed fatigue crack growth in a cast stainless steel pipe elbow. The material tested was equivalent to ASME SA-351CF8M. The David Taylor Research Center (DTRC) was tasked to develop the appropriate material property data to characterize cyclic deformation, cyclic elastic-plastic crack growth and ductile tearing resistance in the pipe elbow material. The tests conducted included monotonic and cyclic tensile tests, monotonic J-R curve tests, and cyclic elastic and elastic-plastic fatigue crack growth rate tests. The cyclic elastic-plastic fracture behavior of the stainless steel was of primary concern and was evaluated using a cyclic J-integral approach. It was found that the cast stainless steel was very resistant to ductile crack extension. J-resistance curves essentially followed a blunting behavior to very high J levels. High cycle fatigue crack growth rate data obtained on this stainless steel was typical of that reported in standard textbooks. Low cycle fatigue crack growth rate data obtained on this material using the cyclic J integral approach was consistent with the high cycle fatigue crack growth rate and with a standard textbook correlation equation typical for this type of material. Evaluation of crack closure effects was essential to accurately determine the crack driving force for cyclic elastic-plastic crack growth in this material.

14. SUBJECT TERMS
Fatigue crack growth rate, Stainless steel, Cyclic, J-integral, crack closure.

15. NUMBER OF PAGES

16. PRICE CODE

17. SECURITY CLASSIFICATION OF REPORT	18. SECURITY CLASSIFICATION OF THIS PAGE	19. SECURITY CLASSIFICATION OF ABSTRACT	20. LIMITATION OF ABSTRACT
UNCLASSIFIED	UNCLASSIFIED	UNCLASSIFIED	SAME AS REPORT